Geoscience Frontiers 4 (2013) 37–56

Contents lists available at SciVerse ScienceDirect

China University of Geosciences (Beijing)

Geoscience Frontiers

journal homepage: www.elsevier.com/locate/gsf

Research paper

Combined U-Pb SHRIMP and Hf isotope study of the Late Paleozoic Yaminué Complex, Rio Negro Province, Argentina: Implications for the origin and evolution of the Patagonia composite terrane

Carlos J. Chernicoff [a,b,*], Eduardo O. Zappettini [b], João O.S. Santos [c,d], Neal J. McNaughton [e], Elena Belousova [f]

[a] National Scientific and Technical Research Council (CONICET), Argentina
[b] Argentine Geological-Mining Survey (SEGEMAR), Argentina
[c] University of Western Australia, Perth, WA 6009, Australia
[d] Redstone Resources, Perth, WA 6849, Australia
[e] John de Laeter Centre, Curtin University, Perth, WA 6102, Australia
[f] ARC National Key Centre for Geochemical Evolution and Metallogeny of Continents (GEMOC), Macquarie University, Sydney, NSW 2109, Australia

ARTICLE INFO

Article history:
Received 23 February 2012
Received in revised form
16 May 2012
Accepted 21 June 2012
Available online 5 July 2012

Keywords:
Yaminué Complex
U-Pb SHRIMP geochronology
Hf isotopes
Tectonics
North Patagonian Massif
Argentina

ABSTRACT

We have carried out zircon U-Pb SHRIMP dating and Hf isotope determinations on a biotite paraschist and on a tonalitic orthogneiss of the Yaminué Complex, and re-evaluate this complex in the broader context of the tectonic evolution of the Patagonia composite terrane. In the metasedimentary unit (msuYC), the youngest detrital zircon dated at 318 ± 5 Ma (Mississippian/Pennsylvanian boundary) indicates a Pennsylvanian (or younger) depositional age. The three main age populations peak at 474, 454 and 374 Ma. Preliminary Hf isotope data for two detrital zircons (447 and 655 Ma) yielded ε(Hf) values of −0.32 and 0.48, indicating that their primary sources contained small amounts of recycled crustal components (of Calymmian age; T_{DM} 1.56 Ga). Zircons from the orthogneiss (miuYC; intrusive into msuYC) show a crystallization age of 261.3 ± 2.7 Ma (Capitanian; late middle Permian) which is broadly coeval with deformation, and Neoarchean–Paleoproterozoic inheritance. Meaningful core-rim relationship between Neoarchean zircon cores and late Permian rims is well defined, indicating the occurrence of Archean crust in this sector of Patagonia. Hf T_{DM} of Permian zircons is mainly Meso-Paleoarchean (2.97–3.35 Ga), with highly negative ε(Hf) values (ca. −33). Hf T_{DM} of inherited Neoarchean zircon cores is also Meso-Paleoarchean (3.14–3.45 Ga) but more juvenile (ε(Hf) = −0.3). Hf isotopes reinforce the presence of unexposed ancient crust in this area.

Combining geological and isotope data, as well as geophysical models, we identify the Yaminué Complex within the La Esperanza-Yaminué crustal block flanked by two other, distinct crustal blocks: the Eastern block which forms part of the Patagonia terrane *sensu stricto*, located in the eastern Patagonian region, and the Western block forming part of the Southern Patagonia terrane. Their origins and timing of amalgamation to form the Patagonia composite terrane are also discussed.

1. Introduction

The southern part of the South American continent, known as the Patagonia region, was previously considered to be an independent and exotic continental fragment with a different geological history from the rest of the South American continent. The tectonic origin(s) of the component parts (terranes/blocks), as well as the timing of amalgamation of the composite terrane (herein referred to as Patagonia composite terrane) and its accretion to the rest of Gondwanaland remains controversial.

* Corresponding author. National Scientific and Technical Research Council (CONICET), Av. Julio A. Roca 651, Piso 8, Buenos Aires, Argentina.
E-mail addresses: jchern@mecon.gov.ar, cc_jorge@yahoo.com.ar (C.J. Chernicoff).

Peer-review under responsibility of China University of Geosciences (Beijing)

Production and hosting by Elsevier

1674-9871/$ – see front matter © 2012, China University of Geosciences (Beijing) and Peking University. Production and hosting by Elsevier B.V. All rights reserved.
http://dx.doi.org/10.1016/j.gsf.2012.06.003

In this study, we utilize combined zircon U-Pb geochronology and Lu-Hf data to evaluate: (1) the basement of what we term herein as the Patagonia terrane (*sensu stricto*) (geographically defined in literature as "Eastern Patagonia" or "Patagonia Oriental"); (2) a newly defined crustal block named La Esperanza-Yaminué; and (3) the Southern Patagonia terrane (as in Ramos, 2010). The age of the Yaminué Complex within the La Esperanza-Yaminué block has important implications for the timing and associated effects of the collision of the Patagonia composite terrane to the rest of the Gondwana continent, since it is located at the northern edge of the Patagonia composite terrane, within what is widely known as the North Patagonian Massif.

The Yaminué Complex (North Patagonian Massif) has been described as a metamorphic unit comprising both igneous and sedimentary protoliths which have been strongly deformed (Caminos, 1983, 2001; Chernicoff and Caminos, 1996a). The dominant rock types are biotite-plagioclase (and/or microcline) schists, tonalitic and granodioritic gneisses, and foliated syntectonic leucogranites, as well as lesser amounts of biotite paraschists, amphibolite and marble. Late- to post- tectonic granitoids have also been described as part of the complex. The first geochronological study of the Yaminué complex yielded whole-rock Rb-Sr errorchrons of 680–620 Ma (Caminos et al., 1994), that were in agreement with the Precambrian age initially assigned to the complex in the first geological maps of the region (Caminos, 1983). These early geochronological data were first challenged by Basei et al. (2002) who obtained conventional U-Pb zircon ages on orthogneisses of the Yaminué Complex at ca. 300 Ma (latest Carboniferous).

Recent studies concentrated on the igneous protoliths of the Yaminué Complex (termed miuYC in our study) (see e.g., Lopez de Luchi et al., 2010; Rapalini et al., 2010; Martinez Dopico et al., 2011, and references therein). No new geochronological data have been presented on the less abundant sedimentary protoliths (termed msuYC in our study). Herein we utilize U-Pb SHRIMP dating of zircons from both the biotite paraschists and orthogneisses of the Yaminué Complex to elucidate their evolution, and Lu-Hf isotope data to characterize their sources. To shed new light on the age and nature of the Yaminué Complex, as well as on its stratigraphic relationship with the surrounding units, we carried out zircon U-Pb SHRIMP dating and Hf isotope determinations on representative samples of a paraschist and an orthogneiss. Our samples of the Yaminué Complex come from exposures in the southern part of the complex (Fig. 1). We report these isotopic data, and discuss their implications in the context of the origin and evolution of the Patagonian region.

2. Geological framework

In this section, a brief description of some of the key geological units exposed in the immediate vicinity of the Yaminué Complex is given, including a partial revision of previous information, encompassing (1) a re-interpretation of the depositional age of the Nahuel Niyeu Formation, and (2) a restriction on the regional validity of the geochronological data of the Navarrete Plutonic Complex. Additionally, the highly reduced exposure of paragneiss/amphibolite recently identified in the Valcheta area (Gozalvez, 2009) is herein given an informal name (Valcheta Gneiss), and assign stratigraphic relevance.

Similarly, as it will be analyzed and discussed further below (see Sections 3 and 6, below), the geochronological data presented in

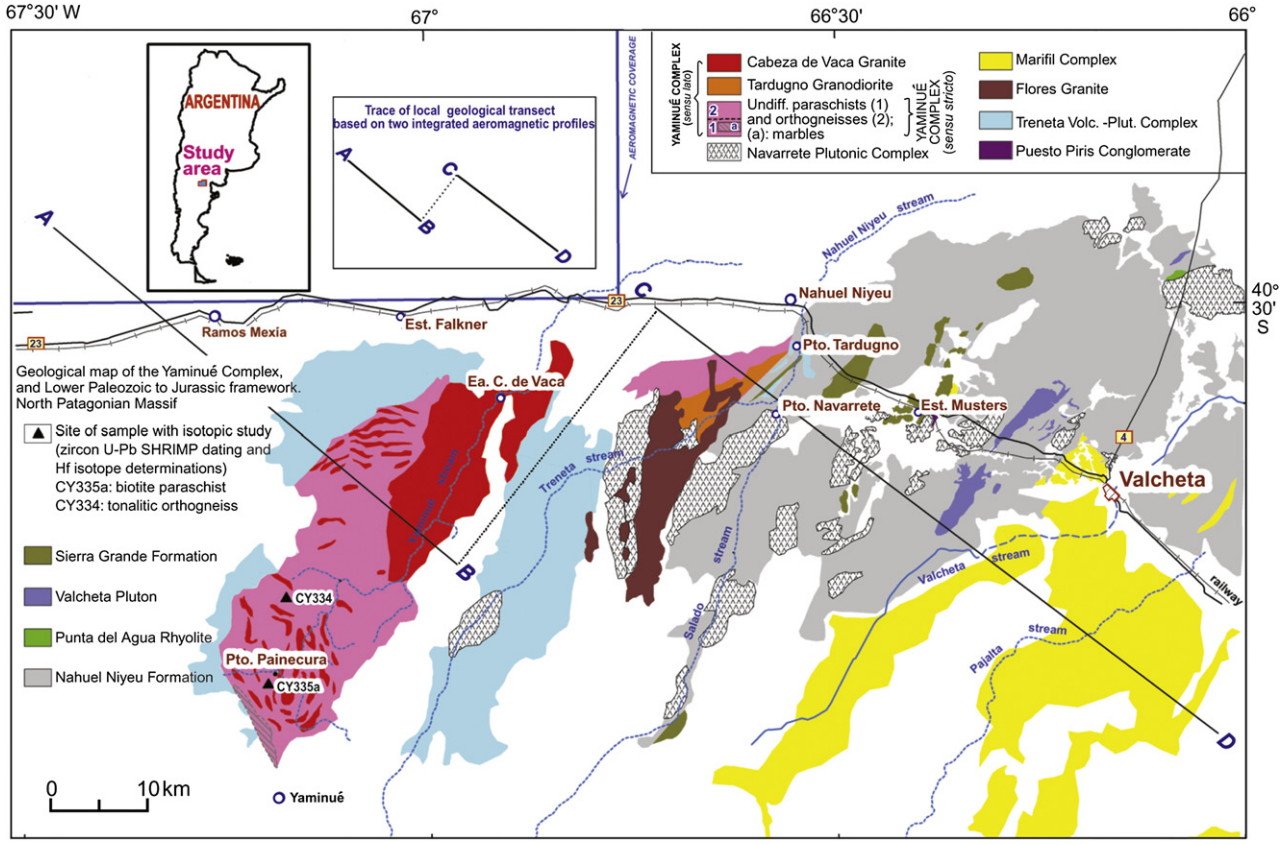

Figure 1. Geological map of the Yaminué-Valcheta area, northern Patagonian region, Argentina. Aeromagnetic coverage is indicated. *ABCD*: trace of two local transects, integrated for modeling (see Fig. 9e). Modified after Chernicoff and Caminos (1996a), and Chernicoff and Gozalvez (2012).

this article entail a re-evaluation of the Yaminué Complex, whose metasedimentary and metaigneous components have yielded the following ages:

(1) Biotite paraschist-paragneiss (metasedimentary unit of the Yaminué Complex—msuYC): youngest detrital zircon dated at ca. 318 Ma (Mississippian/Pennsylvanian boundary) indicates a Pennsylvanian (or younger) depositional age of the protolith, and
(2) Tonalitic orthogneiss (metaigneous unit of the Yaminué Complex—miuYC intrusive into the msuYC): crystallization age of ca. 261 Ma (Capitanian; late middle Permian) roughly coeval with deformation.

The oldest unit in the region is the Nahuel Niyeu Formation (Caminos, 1983; Chernicoff and Caminos, 1996b) which mostly consists of meta-greywackes, shales and phyllites, all of them being unfossiliferous. It has been dated by Pankhurst et al. (2006; zircon U-Pb SHRIMP method) as younger than 515 Ma (youngest peak), but close to this age (i.e. Cambrian Series 2) due to the abundance of coeval zircon grains. In their age estimate, the latter authors disregarded two younger zircons of possible magmatic origin, dated at 482 Ma and 490 Ma, arguing that their age would have resulted from Pb-loss from Cambrian zircons. However, the very low common Pb correction applied to these two analyses (0.05% and 0.10%, respectively) as well as the small degree of discordance, would not allow to interpret these two ages as resulting from Pb-loss. This being the case, the Nahuel Niyeu Formation should be younger than 482 Ma (see Appendix). Otherwise, the Nahuel Niyeu Formation would also be pre-Silurian, taking into account the angular unconformity that separates it from the overlying quartzites assigned to the Silurian—Devonian Sierra Grande Formation (e.g., Caminos, 2001). Additionally, when also considering the intrusive relationship between the Valcheta Pluton (Ar/Ar crystallization age 470 ± 1.8 Ma; Gozalvez, 2009; see also Lopez de Lucchi et al., 2008) and the Nahuel Niyeu Formation, as recently depicted in the geological map of the Estación Muster/Valcheta area (Chernicoff and Gozalvez, 2012), the Nahuel Niyeu Formation should be constrained to the Lower Ordovician. The Nahuel Niyeu Formation is thus considered to be coeval with the newly proposed Polke Formation (Naipauer et al., 2011), formerly included in the Sierra Grande Formation, whose lower- and upper-age limits are 481 and 475 Ma, respectively; the arenaceous and pelitic sediments of the Polke Formation unconformably overlie the El Jagüelito Formation, and subconformably underlie the San Carlos Member of the Sierra Grande Formation.

In the Sierra Grande region (eastern North Patagonian Massif; Fig. 9c), the low-grade metaclastics of the El Jagüelito Formation have generally been regarded as equivalent to the Nahuel Niyeu Formation (e.g., Caminos, 2001 and references therein). However, given the above comments referred to the latter unit, the depositional age of the El Jagüelito Formation would be slightly older. For the meta-greywackes and phyllites, the youngest grain is 510 Ma old and the dominant detrital zircon peak is 538 Ma (zircon U-Pb SHRIMP age; Pankhurst et al., 2006), which would indicate a Cambrian Series 1 age, consistent with trace fossil content (González et al., 2002). As regards the El Jagüelito metaconglomerate, its maximum depositional age would be Late Series 1 to Late Series 3 Cambrian, in agreement with the affinities shown by the archaeocyaths identified in large subangular limestone clasts (González et al., 2011a). Naipauer et al. (2010) have obtained a main zircon age peak at 523 Ma (LA-ICP-MS; youngest age at ca. 503 Ma). The metaluminous Punta Sierra and Arroyo Salado plutons of Sierra Grande area (dated ca. 476 Ma and ca. 475 Ma, respectively; zircon U-Pb SHRIMP,

Figure 2. Meter size recumbent folds in the metaigneous unit of the Yaminué Complex (after Chernicoff, 1994).

Pankhurst et al., 2006) constrain the upper-age limit of the El Jagüelito Formation.

Small exposures of pre-Permian slates, phyllites and siltstones in the northern sector of the North Patagonain Massif (Coli Niyeu Formation, La Esperanza-El Cuy region; Fig. 9c), have been correlated with the Nahuel Niyeu Formation (Bjerg et al., 1997; Saini-Eidukat et al., 1999).

The strongly peraluminous Valcheta Pluton (Gozalvez, 2009) is bound to intrude the Nahuel Niyeu Formation (Fig. 1) and is regarded to derive by partial melting of sedimentary rocks. The occurrence of large enclaves of banded gneiss and amphibolite (see e.g., Fig. 2b in Gozalvez, 2009) in this pluton does not support the low-grade metasedimentary rocks of the Nahuel Niyeu Formation to be their original rock unit but, rather, an unexposed and most likely underlying higher-grade basement herein informally referred to as the Valcheta Gneiss. The protolith of the Valcheta Gneiss is bound to be older than ca. 470 Ma, and could well share the same depositional age with the protolith of the Mina Gonzalito Gneiss. A small volume of Valcheta Gneiss-derived anatectic melt (i.e. part of the Valcheta Pluton) is bound to have ascended possibly via fractures so as to reach the Nahuel Niyeu Formation, as depicted in Fig. 9e, though no contact metamorphism resulting from this

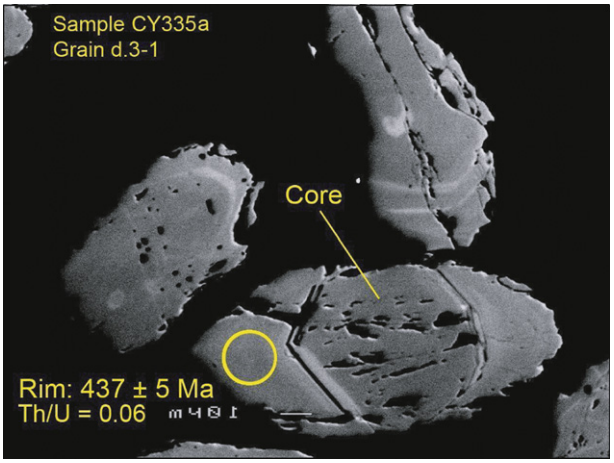

Figure 3. BSE (back-scattered electrons) image of zircon d.3-1 of sample CY335a (metasedimentary unit of the Yaminué Complex; biotite paraschist). The metamorphic rim is dated at 437 ± 5 Ma (Silurian, Llandovery) whereas the core remains undated because the presence of a cluster of inclusions.

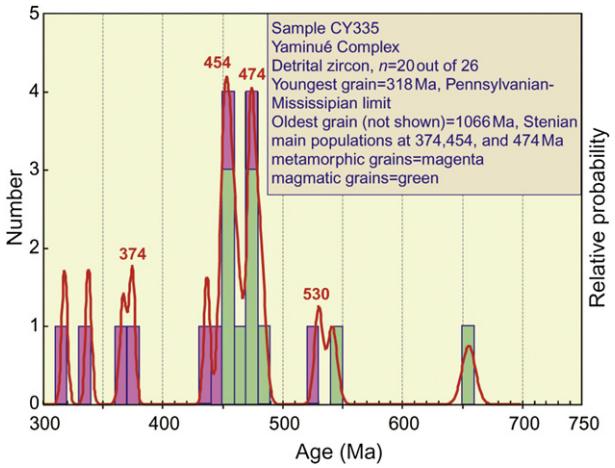

Figure 4. Cumulative probability plot of $^{206}Pb/^{238}U$ isotopic ages of detrital zircons ($n = 20$ out of 26) from the metasedimentary unit of the Yaminué Formation (biotite paraschist, sample CY335a). One Mesoproterozoic age is not shown. Youngest grain: 318 ± 5 Ma.

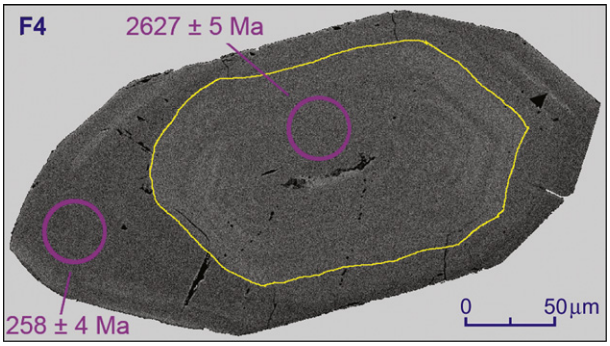

Figure 6. BSE (back-scattered electrons) image of zircon F4 of sample CY334 (tonalitic orthogneiss; metaigneous unit of the Yaminué Complex) showing older magmatic Neoarchean core (2627 ± 5 Ma) and Permian magmatic rim (258 ± 4 Ma).

envisaged stratigraphic relationship has yet been identified, and further studies are still pending (Gozalvez, 2009).

As pointed out by Gozalvez (2009), an analogous relationship between granitic magma segregation (Tapera and María Teresa plutons) and gneiss-amphibolite (Mina Gonzalito Gneiss) occurs about 100 km towards the southeast, in the exposures of the Sierra Grande region (eastern North Patagonian Massif). In the latter region, the metamorphic peak age of the Mina Gonzalito Gneiss has been dated at ca. 472 Ma (Pankhurst et al., 2006) and its protoliths may be late Neoproterozoic to early Cambrian (e.g., Dalla Salda et al., 2003) or constrained to the Cambrian, Series 1 (Pankhurst et al., 2006). The Valcheta Gneiss is likely to be equivalent to the Mina Gonzalito Gneiss, and to underlie the Nahuel Niyeu Formation. From the much younger age herein obtained for the metasedimentary unit of the Yaminué Complex (see below), it follows that the latter unit cannot be equivalent either to the Mina Gonzalito Gneiss or to the Valcheta Gneiss. The igneous-metamorphic Las Grutas Complex (González et al., 2008) exposed along the Atlantic coast would be equivalent to the Mina Gonzalito Complex.

The Valcheta Pluton, as well as the Tapera and María Teresa plutons, are geochemically distinct from the mostly metaluminous, Ordovician (but slightly older) intrusive rocks exposed in the Sierra Grande region (e.g., Punta Sierra Plutonic Complex; Busteros et al., 1998); the relationship between the former and the latter groups has still not been investigated.

As said before, unfossiliferous and undated quartzites and minor conglomerates exposed at the Valcheta area (Sierra Grande Formation), unconformably overlie the Nahuel Niyeu Formation, and have been correlated (e.g., Caminos, 2001) with the fossiliferous Silurian–Devonian sediments exposed at the type area, where the youngest detrital zircon has been dated at 428 Ma (LA-ICP-MS; Uriz et al., 2010).

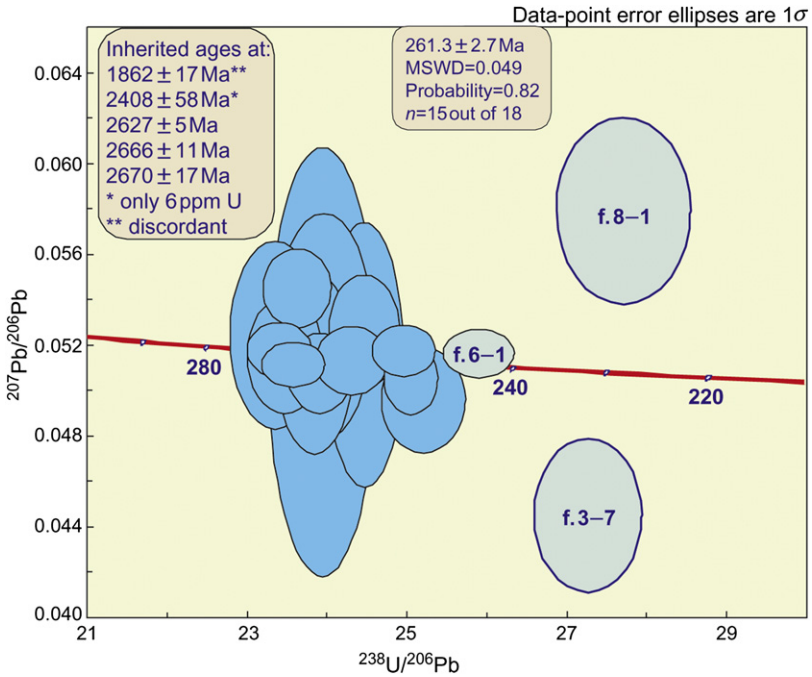

Figure 5. Inverse concordia plot ($^{207}Pb/^{206}Pb$ vs. $^{238}U/^{206}Pb$) of zircon from the metaigneous unit of the Yaminué Complex (sample CY334, tonalitic orthogneiss). The age of zircon pools at 261.3 ± 2.7 Ma (MSWD = 0.049).

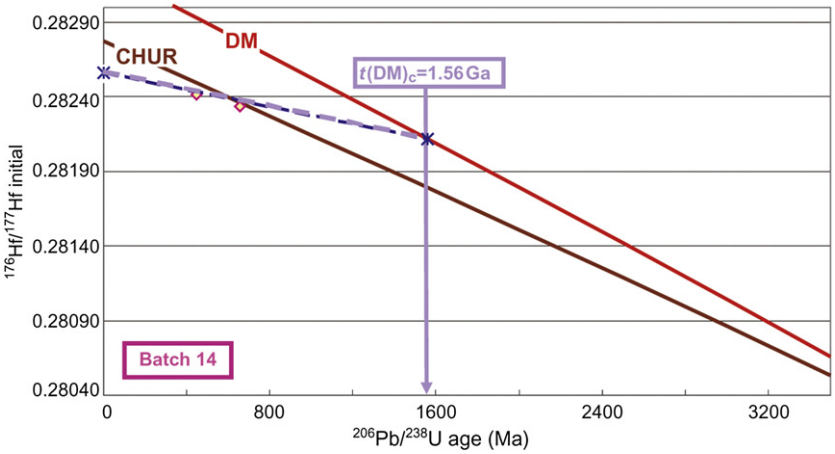

Figure 7. Diagram of $^{176}Hf/^{177}Hf$ (initial) vs. $^{206}Pb/^{238}U$ ages of two zircons of sample CY335a (biotite paraschist), metasedimentary unit of the Yaminué Complex. The depleted mantle model-age (crustal) is early Mesoproterozoic (1.56 Ga; Calymmian). The slope of the dashed line uses the ratio of 0.015 for the $^{176}Lu/^{177}Hf$ ratio.

The Navarrete Plutonic Complex (Caminos, 1983, 2001) is a large granitic unit exposed at the Valcheta area. A granodiorite sampled at Puesto Navarrete (66°35′W/40°35′S; Fig. 1) has been dated at 281 ± 3 Ma (zircon U-Pb SHRIMP; Pankhurst et al., 2006), the latter authors having assigned this age to the entire Complex. A large portion of the western outcrops of the Navarrete Complex (west of ca. 66°55′W) have recently been re-mapped as part of the Yaminué Complex granitic orthogneisses (or late tectonic granites, referred to as Cabeza de Vaca Granite, by López de Lucchi et al., 2010). However, a remaining part of them (east of ca. 66°55′W) has been kept as part of the Navarrete Complex, as originally mapped (Caminos, 2001). Since in the present work, we have dated the Yaminué Complex orthogneisses at ca. 261 Ma (see below), it follows that they cannot be intruded by Navarrete Complex magmatic rocks at 281 Ma. Hence, we herein restrict the validity of the latter age only to the type area of the Navarrete Complex at Puesto Navarrete and other exposures to the south and east, but not to its former —still undated— "western outcrops", the whole of which should pertain to the Yaminué Complex metaigneous unit (and/or Cabeza de Vaca Granite). Indeed, the contacts between the Cabeza de Vaca Granite and the former "western outcrop" of the Navarrete Complex has been described to be transitional at fine scale (López de Lucchi et al., 2010) possibly because they should both belong to a single unit (i.e. late tectonic stage of the Yaminué Complex metaigneous unit).

In spite of the small age difference between the metasedimentary and metaigneous units of the Yaminué Complex, in this paper we prefer to maintain the encompassing term "Yaminué Complex" because since these two components are jointly and intimately folded and thrust in several scales, it has not been possible to map them separately. Additionally, the exposures of the metasedimentary unit are much more restricted than those of the metaigneous unit.

The metasedimentary unit of the Yaminué Complex mostly comprises biotite (muscovite) paraschist-paragneisses, a sample of which has been dated herein, therefore the age of the host rocks of the foliated granitoids and orthogneisses of the Yaminué Complex is no longer unknown. The metaigneous rock sample dated herein is a tonalitic orthogneiss (see Section 3, below). What still remains unconfirmed is the depositional age of the protolith of the marbles exposed in the southwestern corner of the Yaminué Complex (Caminos, 2001); in-progress C- and O-isotope study carried out by the present authors has still not indicated a definitive age range. The marbles and minor amphibole schists crop out mostly as a NW trending belt (10 km long, 1.5 km wide) that is parallel to, and conform with the schistosity of the southern exposures of the

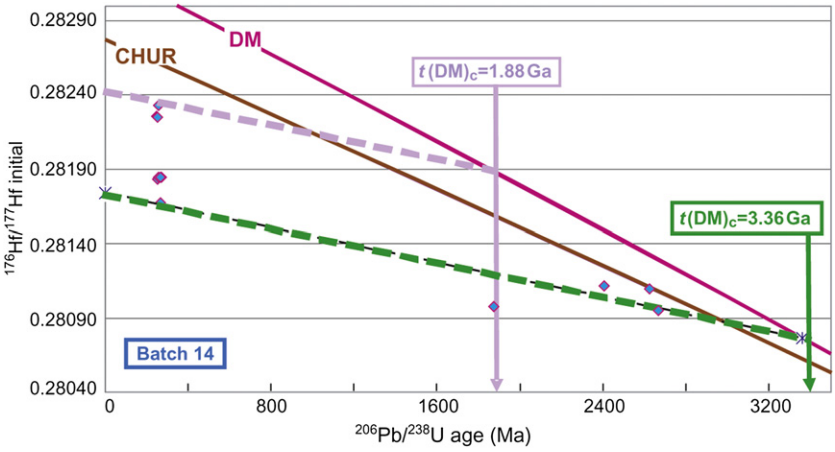

Figure 8. Diagram of $^{176}Hf/^{177}Hf$ (initial) vs. $^{206}Pb/^{238}U$ ages of dated zircons of sample CY334 (tonalitic orthogneiss), metaigneous unit of the Yaminué Complex. The depleted mantle model-age (crustal) are Paleoarchean (3.36 Ga) and middle Paleoproterozoic (1.88 Ga; Orosirian). The slope of the dashed line uses the ratio of 0.015 for the $^{176}Lu/^{177}Hf$ ratio.

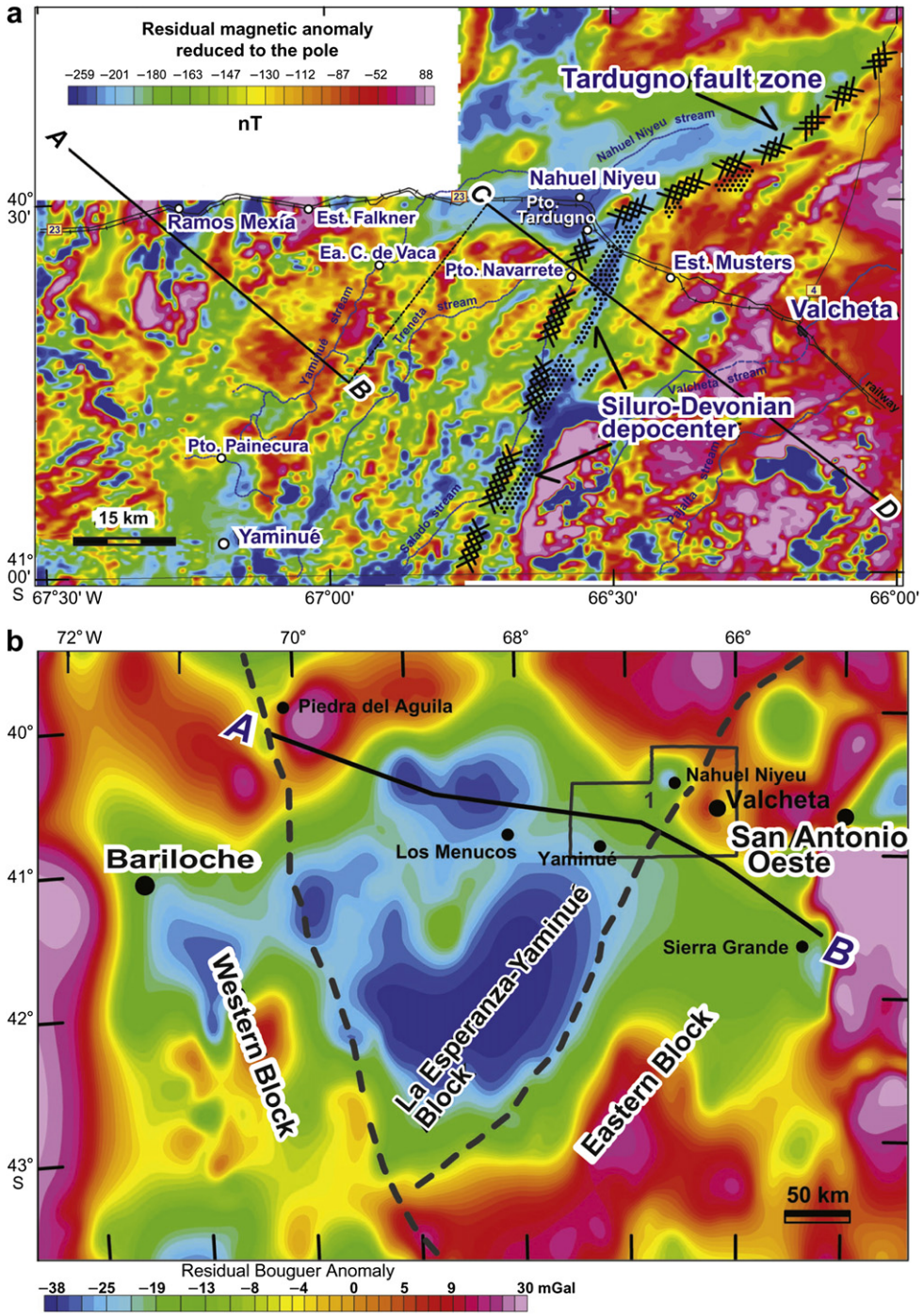

Figure 9. (a) Aeromagnetic survey map (total magnetic intensity reduced to the pole) of the Yaminué-Valcheta area, northern Patagonian region, with trace of integrated, NW-SE geological-geophysical transect (*ABCD*). (b) Bouguer residual anomaly map of a larger portion of the northern Patagonian region, with trace of a WNW-ESE geological-geophysical transect. 1: area with aeromagnetic coverage (a); *AB*: modeled transect. (c) Simplified geology, and locality map of the gravimetric transect. References (of Fig. 9c): 1: Mina Gonzalito Gneiss, 2: El Jagüelito Formation, 3: Nahuel Niyeu + Coli Niyeu formations, 4: Punta Sierra Plutonic Complex, 5: Sierra Grande Formation, 6: Yaminué Complex, 7: La Esperanza Complex, Mamil Choique and equivalent Permian granitoids, 8: Treneta Complex and equivalents, 9: Flores Granite, 10: Marifil Complex and Lonco Trapial Formation, 11: undifferentiated Cretaceous–Cenozoic sediments, 12: Quaternary basalts. (d) Geological model of the gravimetric data. (e) Geological model of the aeromagnetic data. References (of Fig. 9e): YCms: metasedimentary unit of the Yaminué Complex (paraschist-paragneiss), YCm: metasedimentary unit of the Yaminué Complex (marbles), YCmi: metaigneous unit of the Yaminué Complex, Tg: metaigneous unit of the Yaminué Complex (Tardugno Granodiorite), SG: Sierra Grande Formation, Ng: Navarrete Plutonic Complex, Van: Valcheta Pluton (anatexite), NN+EJ: Nahuel Niyeu and El Jagüelito formations, MG: Mina Gonzalito Gneiss, EBB: Eastern block basement, Tv: Treneta volcanics, Sb: Somuncura basalts. Aeromagnetic data processed after SEGEMAR (2005); profiles extracted from the aeromagnetic grid at a sampling interval of 250 m. Gravity data correspond to a subset of the 1 km gravimetric grid of Argentina, made available by the Instituto de Física de Rosario to SEGEMAR (Geological Survey of Argentina), and further processed into a residual Bouguer anomaly grid by substracting a 35 km-upward continued gravity grid from the unfiltered grid. For both aeromagnetics and gravimetry, the commercial modeling software package used is ModelVision™.

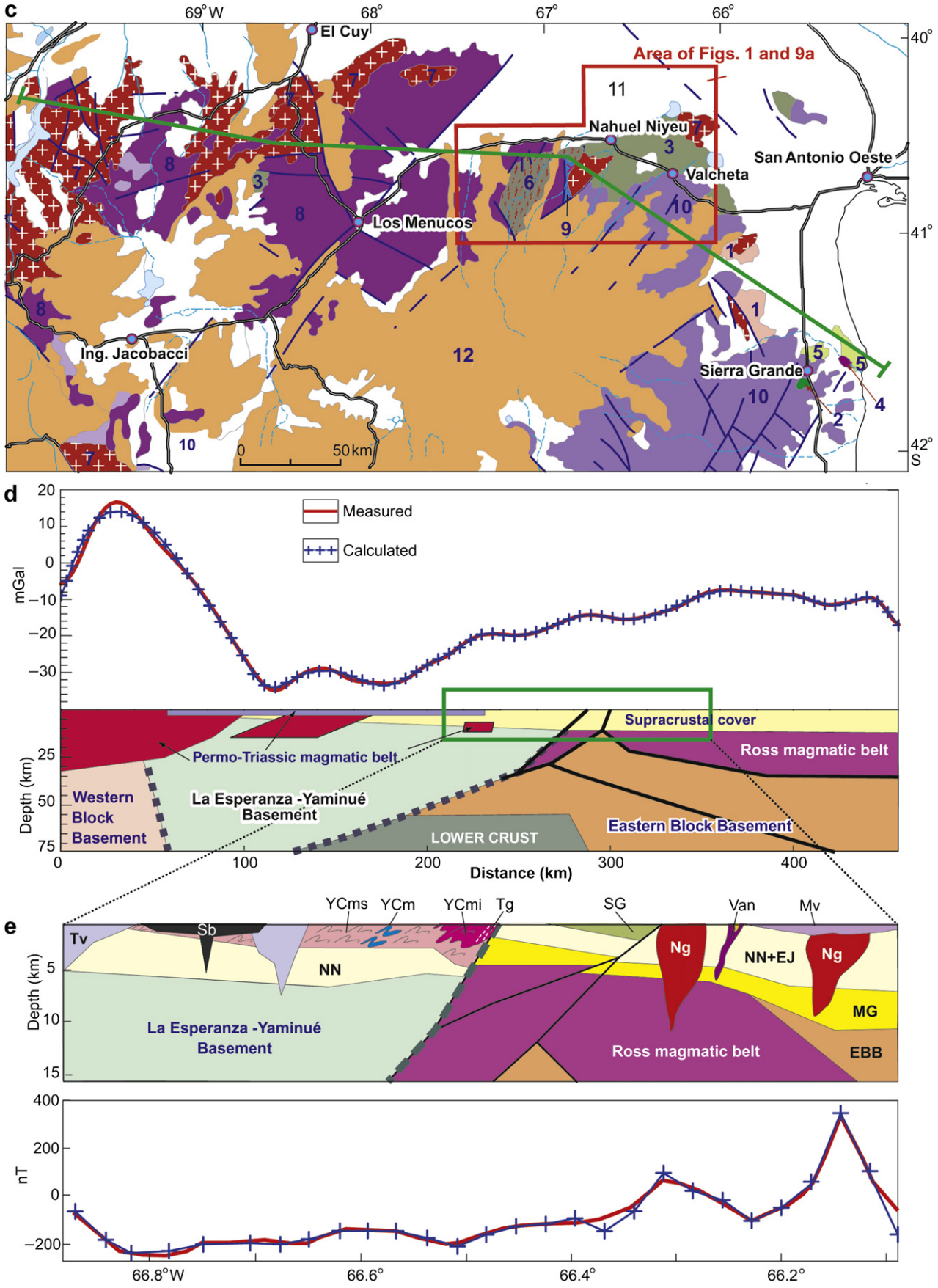

Figure 9. (*continued*).

Yaminué Complex and, as such, they are bound to pertain to the metasedimentary unit of the Yaminué Complex—msuYC. The whole of the msuYC, i.e. predominant epiclastic metasediments and subordinate marbles, is herein regarded to pertain to a single basin, the context of which is referred to in Section 7, below.

The metaigneous unit of the Yaminué Complex mostly comprises syn-kinematic granitoids and orthogneisses of granodioritic and tonalitic composition, as well as late kinematic leucogranites; (see detailed, updated petrography given by López de Lucchi et al., 2010). The Tardugno Granodiorite, which is also a late kinematic intrusive of the Yaminué Complex, isolated from its main area of outcrops, is in tectonic contact with the Nahuel Niyeu Formation (Chernicoff and Caminos, 1996a) along an NE trending fault zone that is also recognizable in the regional aeromagnetic images (see "Tardugno fault zone" east of Pto. Tardugno, indicated in Fig. 9a; see also Section 4, below). In the context of the microstructures of the metaigneous unit of the Yaminué Complex being indicative of a transition from magmatic to solid-state deformation (López de Lucchi et al., 2010), hence pointing to an emplacement under a continuous decreasing temperature, the consistent parallelism between the foliation of the metaigneous unit of the Yaminué Complex and the schistosity of the metasedimentary unit of the Yaminué Complex, attest to the overall syn-kinematic nature of the metaigneous unit, this characteristic being less valid for the late kinematic leucogranites.

The Yaminué Complex as a whole has a most conspicuous feature that stands out at various scales, that is its sub-horizontal to gentle dipping foliation/schistosity planes, mimicked by the flat topography. The joint deformation of the metasedimentary and metaigneous units of the Yaminué Complex involves an early folding stage transitionally succeeded by a late thrusting stage (Chernicoff and Caminos, 1996a). Folding is tight and mostly recumbent, and is developed at several scales from decimeter to decameter scales, only and rarely standing out in the metaigneous component (see Fig. 2). For most part of the complex, the thrust planes along which the syn- to late-kinematic sheet-like intrusions accommodated, are also sub-horizontal. The Fig. 14a of López de Lucchi (2010) has sketched the latter relationship, although the host should be the biotite paraschist herein referred to as the metasedimentary unit of the Yaminué Complex (i.e., not the Nahuel Niyeu Formation), and the age of the deformation should be around 261 Ma (this article).

In spite of the sub-horizontal character of the "D1" planar fabrics, their strike and dip could still be systematically measured in the field, NW to WNW, together with the roughly perpendicular mineral lineations, NE to ENE, these readings being particularly reliable in the northern exposures of the Yaminué Complex, less affected by the superimposed, "D2" northerly trending and sub-horizontally plunging folds (Chernicoff and Caminos, 1996a). Particularly visible in the southern outcrops of the Yaminué Complex, "D2" would have caused the twist of the "D1" planar fabric towards the NNW, and that of the "D1" mineral lineations roughly towards the ENE. The conventional, field structural measurements have lately been confirmed by AMS measurements (anisotropy of magnetic susceptibility; López de Lucci et al., 2010), all in all establishing a main NNE-SSW compressional event associated with top-to-the-SSW thrusting. Such tectonic scenario is analogous to that envisaged by von Gosen (2003) for the whole of the northern Patagonian region during Late Paleozoic times (see Section 7. Tectonic evolution, Permian). The Tardugno Granodiorite would have been emplaced during the late "D1" stage, in accordance with the occurrence of mylonitization developed heterogeneously throughout the pluton (Chernicoff and Caminos, 1996a).

The latest pre-Cenozoic magmatic units in the region are the Treneta Plutonic-Volcanic Complex and the Marifil Volcanic Complex. The former includes both Triassic (?) lavas and ignimbrites of intermediate composition, and early Jurassic leucogranites (Flores Granite) dated at ca. 188 Ma (Rb-Sr isochron, Pankhurst et al., 1993; and muscovite K-Ar cooling age, López de Luchi et al., 2008), respectively covering unconformably or intruding the Navarrete Plutonic Complex (Caminos, 1983, 2001). Near Valcheta and more extensively exposed near Sierra Grande, the middle Jurassic Marifil Volcanic Complex comprises rhyolitic and dacitic ignimbrites, and rhyolitic and granitic porphyries (Caminos, 2001).

3. Isotopic data

The combination of U-Pb SHRIMP and Hf isotopic determinations for individual zircon grains provides not only the age but the nature and source of the host magma, whether crustal or juvenile mantle, and model age (T_{DM}) of the provenance. This integrated analysis, applied to suites of detrital zircon, gives a more distinctive, and more easily interpreted, picture of crustal evolution in the provenance area than age data alone (Veevers et al., 2006 and references therein).

3.1. U-Pb SHRIMP geochronology

3.1.1. Methodology

Samples CY335a (biotite paraschist) and CY334 (tonalitic orthogneiss) were collected in the southern exposures of the Yaminué Complex (see Fig. 1). The rocks were crushed, milled, sieved at 60 mesh, and washed to remove the clay and silt fractions. The remaining material, corresponding to fine sand and very fine sand, was dried and processed by two heavy liquids: LST (lithium-sodium tungstate, density 2.8) and TBE (tetra-bromo-ethane, density 3). The heavy mineral concentrates were separated into four fractions using a Frantz® magnetic separator. Zircon grains were picked from the least magnetic fraction at 1 A and 5° inclination and then mounted in an epoxy disc of 2.5 cm diameter together with the analytical standards. The mount was polished and coated with carbon for imaging using a JEOL6400 Scanning Electron Microscope at the Centre for Microscopy, Characterization and Microanalyses of the University of Western Australia. This carbon coat was removed and replaced for a gold coating for SHRIMP U-Pb analyses.

Sensitive High Mass Resolution Ion MicroProbe (SHRIMP II) U-Pb analyses were performed at Curtin University in two sessions using an analytical spot size of about 20–25 μm. Individual analyses are composed of measurement of nine masses repeated in five scans. The following masses were analyzed for zircon: (Zr_2O, ^{204}Pb, background, ^{206}Pb, ^{207}Pb, ^{208}Pb, ^{238}U, ^{248}ThO, ^{254}UO). The standards D23 and NBS611 were used to identify the position of the peak of the mass ^{204}Pb, whereas the calibration of the U-content and the Pb/U ratio were done using the zircon standard BR266 (559 Ma, 903 ppm U). Data were reduced using the SQUID© 1.03 software (Ludwig, 2001) and the ages calculated using Isoplot© 3.0 (Ludwig, 2003). The Phanerozoic ages are mean average $^{206}Pb/^{238}U$ ages whereas the Precambrian ages are mean average $^{207}Pb/^{206}Pb$ ages all calculated at 2σ level. The individual analyses are quoted at 1σ level (Table 1).

3.1.2. Results

3.1.2.1. Sample CY335a (biotite paraschist). Twenty-six detrital zircons were analyzed with the SHRIMP to determine the ages of the major sources for the sedimentary deposition. Six of these zircons showed discordance of 10% or more, whereas the remaining data are considered to reliably reflect the ages of zircon formation. Most of the near-concordant grains are Ordovician ($n = 11$) or Lower Silurian–Devonian ($n = 3$) in age, followed by Cambrian

Table 1
Isotopic data (U-Pb and Hf) of zircons of biotite paraschist (sample CY335a) and tonalitic orthogneiss (sample CY334), Yaminué Complex.

Spot	U (ppm)	Th/U	4f206 (%)	Isotopic ratios					Age (Ma)		Disc. %	Hf	ε(Hf)
				$^{207}Pb/^{206}Pb$	$^{207}Pb/^{235}U$	$^{206}Pb/^{238}U$	Error corr.	$^{208}Pb/^{232}Th$	$^{206}Pb/^{238}U$	$^{207}Pb/^{206}Pb$		$T_{DM(c)}$ (Ma)	
Sample CY335 (biotite paraschist)													
b.1-1	535	0.01	0.76	0.05298 ± 5.56	0.3932 ± 5.74	0.0538 ± 1.45	0.253	–	338 ± 5	328 ± 126	−3		
b.2-2	502	0.01	0.42	0.05526 ± 3.00	0.5552 ± 3.29	0.0729 ± 1.37	0.416	–	453 ± 6	423 ± 67	−7		
b.2-3	393	0.02	0.45	0.05605 ± 3.10	0.5882 ± 3.40	0.0761 ± 1.40	0.412	0.0191 ± 88.08	473 ± 6	455 ± 69	−4		
b.4-3	556	0.55	0.04	0.07492 ± 0.73	1.8848 ± 1.48	0.1824 ± 1.29	0.869	0.0540 ± 1.54	1080 ± 13	1066 ± 15	−1		
b.4-4	183	0.29	0.36	0.05694 ± 3.73	0.5992 ± 4.06	0.0763 ± 1.62	0.398	0.0232 ± 5.97	474 ± 7	489 ± 82	3		
b.4-5	242	0.35	1.79	0.05582 ± 7.04	0.5665 ± 7.22	0.0736 ± 1.57	0.217	0.0220 ± 10.03	458 ± 7	445 ± 157	−3		
b.5-1	630	0.00	0.42	0.05561 ± 2.79	0.5564 ± 3.10	0.0726 ± 1.34	0.433	–	452 ± 6	437 ± 62	−3		
b.5-2	274	0.86	0.27	0.05652 ± 4.05	0.6018 ± 4.31	0.0772 ± 1.49	0.345	0.0243 ± 2.84	480 ± 7	473 ± 90	−1		
b.10-1	183	0.40	1.91	0.06748 ± 8.23	0.7177 ± 8.40	0.0771 ± 1.69	0.201	0.0283 ± 9.43	479 ± 8	853 ± 171	44		
b.11-1	509	0.01	1.13	0.05309 ± 8.40	0.3700 ± 8.54	0.0505 ± 1.57	0.184	–	318 ± 5	333 ± 190	4		
b.12-1	507	0.01	2.43	0.05672 ± 6.55	0.4581 ± 6.71	0.0586 ± 1.44	0.215	–	367 ± 5	481 ± 145	24		
d.1-1	235	0.97	0.13	0.05621 ± 2.25	0.6030 ± 2.77	0.0778 ± 1.61	0.581	0.0237 ± 2.11	483 ± 7	461 ± 50	−5		
d.1-2	300	0.56	0.00	0.05606 ± 1.75	0.5894 ± 2.25	0.0762 ± 1.41	0.627	0.0230 ± 2.04	474 ± 6	455 ± 39	−4		
d.1-3	285	0.01	0.81	0.05451 ± 5.49	0.4495 ± 5.65	0.0598 ± 1.34	0.237	0.0637 ± 46.51	374 ± 5	392 ± 123	5		
d.2-1	195	0.18	0.00	0.05721 ± 2.07	0.6910 ± 2.63	0.0876 ± 1.63	0.620	0.0265 ± 3.41	541 ± 8	500 ± 46	−8		
d.3-1	491	0.01	0.22	0.05612 ± 1.97	0.5425 ± 2.31	0.0701 ± 1.21	0.524	–	437 ± 5	457 ± 44	4		
d.4-1	335	0.16	0.01	0.05827 ± 1.49	0.6884 ± 2.00	0.0857 ± 1.33	0.667	0.0261 ± 3.42	530 ± 7	540 ± 33	2		
d.4-2	58	0.78	0.00	0.06357 ± 3.22	0.9378 ± 3.69	0.1070 ± 1.80	0.487	0.0335 ± 2.78	655 ± 11	727 ± 68	10	1620	0.48
d.5-1	313	0.69	0.00	0.05910 ± 1.76	0.5738 ± 2.25	0.0704 ± 1.40	0.622	0.0229 ± 5.28	439 ± 6	571 ± 38	23		
d.6-1	173	0.56	0.00	0.05559 ± 2.50	0.5714 ± 2.89	0.0746 ± 1.46	0.504	0.0229 ± 2.50	464 ± 7	436 ± 56	−6		
d.6-2	301	0.47	0.62	0.05688 ± 3.30	0.5759 ± 3.66	0.0734 ± 1.58	0.430	0.0250 ± 3.38	457 ± 7	487 ± 73	6		
d.7-1	140	0.63	0.00	0.05809 ± 2.49	0.6001 ± 2.96	0.0749 ± 1.59	0.538	0.0237 ± 2.50	466 ± 7	533 ± 55	13		
d.8-1	472	0.01	3.04	0.05695 ± 6.04	0.5189 ± 6.18	0.0661 ± 1.30	0.210	–	413 ± 5	490 ± 133	16		
d.8-2	433	0.01	0.13	0.05879 ± 2.61	0.5827 ± 2.89	0.0719 ± 1.25	0.432	0.0626 ± 21.60	447 ± 5	559 ± 57	20	1540	−0.32
d.9-1	375	0.07	1.98	0.05451 ± 6.68	0.4404 ± 6.88	0.0586 ± 1.67	0.242	0.0209 ± 39.30	367 ± 6	392 ± 150	6		
d.9-2	310	0.83	2.61	0.05595 ± 8.07	0.5556 ± 8.19	0.0720 ± 1.42	0.173	0.0216 ± 5.19	448 ± 6	450 ± 179	0		
Sample CY334 (tonalitic orthogneiss)													
f.1-1	373	0.31	0.05	0.05114 ± 1.60	0.2988 ± 2.12	0.0424 ± 1.39	0.656	0.0136 ± 2.11	267 ± 4	247 ± 375	−8	3350	−32.92
f.1-2	413	0.60	0.04	0.05177 ± 1.92	0.3048 ± 2.38	0.0427 ± 1.41	0.592	0.0137 ± 2.02	269 ± 4	275 ± 44	2		
f.1-3	116	0.48	0.34	0.05120 ± 6.34	0.2958 ± 6.56	0.0419 ± 1.67	0.255	0.0130 ± 5.63	265 ± 4	250 ± 146	−6		
f.1-4	93	0.25	−0.01	0.18147 ± 0.69	11.812 ± 1.65	0.4721 ± 1.50	0.908	0.1167 ± 3.53	2493 ± 31	2666 ± 11	7		
f.2-1	62	0.48	0.61	0.05158 ± 9.24	0.2904 ± 9.39	0.0408 ± 1.63	0.174	0.0122 ± 8.52	258 ± 4	267 ± 212	3	1920	−9.96
f.2-2	184	1.17	0.25	0.04955 ± 3.82	0.2709 ± 4.18	0.0397 ± 1.69	0.405	0.0121 ± 2.79	251 ± 4	174 ± 89	−44	3020	−27.74
f.2-3	534	0.11	0.04	0.05049 ± 2.57	0.2777 ± 2.80	0.0399 ± 1.12	0.400	0.0118 ± 4.87	252 ± 3	218 ± 59	−16		
f.3-1	304	0.78	0.21	0.05075 ± 2.79	0.2926 ± 3.10	0.0418 ± 1.36	0.439	0.0127 ± 2.22	264 ± 4	230 ± 64	−15		
f.3-2	70	0.26	0.83	0.05281 ± 7.69	0.3037 ± 7.95	0.0417 ± 2.03	0.256	0.0102 ± 13.71	263 ± 5	321 ± 175	18		
f.3-3	93	0.65	0.16	0.05244 ± 6.44	0.3037 ± 6.70	0.0420 ± 1.85	0.276	0.0124 ± 5.00	265 ± 5	305 ± 147	13		
f.3-4	178	0.11	−0.09	0.11456 ± 0.94	3.3463 ± 1.81	0.2119 ± 1.55	0.856	0.0663 ± 2.95	1239 ± 17	1873 ± 17	34	3910	−21.78
f.3-5	313	0.56	0.00	0.05129 ± 2.40	0.2907 ± 2.83	0.0411 ± 1.50	0.532	0.0131 ± 2.39	260 ± 4	254 ± 55	−2		
f.3-6	155	0.76	0.35	0.05156 ± 4.04	0.3026 ± 4.37	0.0426 ± 1.67	0.382	0.0124 ± 3.13	269 ± 4	266 ± 93	−1	2980	−26.83
f.3-7	304	0.25	0.99	0.04451 ± 6.20	0.2249 ± 6.51	0.0367 ± 2.01	0.309	0.0116 ± 4.5	232 ± 4	−83 ± 152	381		
f.4-1	111	0.19	0.00	0.05256 ± 3.86	0.2960 ± 4.14	0.0408 ± 1.50	0.362	0.0133 ± 5.10	258 ± 4	310 ± 88	17	2990	−27.21
f.4-2	455	0.72	0.02	0.17723 ± 0.31	11.565 ± 1.08	0.4732 ± 1.03	0.959	0.1270 ± 1.12	2498 ± 21	2627 ± 5	5	3140	−0.30
f.5-1	331	0.31	0.00	0.18184 ± 1.04	12.168 ± 1.45	0.4853 ± 1.02	0.702	0.1297 ± 1.55	2550 ± 22	2670 ± 17	4	3450	−4.53
f.6-1	614	0.13	−0.03	0.05162 ± 1.69	0.2746 ± 2.19	0.0386 ± 1.39	0.636	0.0121 ± 3.34	244 ± 3	268 ± 39	9	2090	−12.83
f.6-2	6	0.29	0.00	0.15559 ± 3.41	8.8488 ± 4.95	0.4125 ± 3.59	0.725	0.1247 ± 7.31	2226 ± 67	2408 ± 58	8	3250	−4.69
f.6-3	46	0.74	0.74	0.05124 ± 15.1	0.2949 ± 15.3	0.0417 ± 2.31	0.151	0.0128 ± 9.44	264 ± 6	251 ± 347	−5		
f.7-1	146	0.63	0.00	0.05448 ± 2.57	0.3178 ± 2.97	0.0423 ± 1.48	0.499	0.0135 ± 2.77	267 ± 4	391 ± 58	32	2980	−26.93
f.7-2	440	1.25	0.00	0.05175 ± 1.78	0.2856 ± 2.19	0.0400 ± 1.28	0.583	0.0121 ± 1.80	253 ± 3	275 ± 41	8	2100	−12.98
f.8-1	82	0.11	0.00	0.05790 ± 5.81	0.2880 ± 6.32	0.0361 ± 2.49	0.395	0.0117 ± 11.0	228 ± 6	526 ± 127	57		

[Series 1 (Terreneuvian); $n = 2$], Carboniferous ($n = 2$), Cryogenian ($n = 1$), late Neoproterozoic ($n = 1$) and Mesoproterozoic (Stenian, $n = 1$). Fifteen grains are interpreted as magmatic, whereas eleven display metamorphic rims (e.g., b.1-1, b.2-2, b.5-1, b.11-1, b.12-1, d.1-3, d.3-1, d.8-1, and d.8-2; see Fig. 3) or zones (b.2-3 and d.9-1).

The interpreted metamorphic grains/zones generally have Th/U ratios of 0.01 or less, much lower than the magmatic grains/areas (0.16–0.97). The proportion of metamorphic zircons (rims and zones) is high (i.e. 41%), which may reflect the relative abundance of metamorphic rocks in the source area for the interpreted immature sedimentary protolith (greywacke?). There is a dominance of metamorphic zircons with ages of middle late Ordovician (447–453 Ma) and there are other metamorphic grains/areas formed during Lower Silurian (437 Ma), Lower Devonian (413 Ma), Upper Devonian (367 and 375 Ma), and Carboniferous (338 and 318 Ma). This indicates the occurrence of several pulses of metamorphism in the source areas. The metamorphic grade should be amphibolite facies or higher to be capable to re-crystallize zircon. Such source areas were probably proximal at the time of sediment deposition as metamorphic grains tend to survive less well during transport and recycling when compared to magmatic grains, because on average they are richer in U (e.g., Hartmann and Santos, 2004).

Since the metamorphic grade of the biotite paraschist does not exceed that of lower amphibolite (where zircon recrystallization is unlikely), this means that even the youngest metamorphic zircon grain (318 Ma) would be detrital, hence indicating a Pennsylvanian (or younger) depositional age for the sedimentary protolith.

The cumulative probability plot (Fig. 4) shows three main age populations at ca. 374 Ma ($n = 2$), 454 Ma ($n = 5$) and 474 Ma ($n = 7$).

The main source of the metasedimentary sequence is represented by Ordovician zircons. About two-thirds of the Ordovician zircons are magmatic and one-third is metamorphic. Potential magmatic sources are located in the eastern Patagonian region, such as: (1) the Mina Gonzalito Gneiss and equivalents, with a metamorphic peak dated at ca. 472 Ma, and a series of plutons pertaining to the Punta Sierra Plutonic Complex dated at ca. 475 Ma in the Sierra Grande area. In both cases, the dating method was U-Pb in zircons by SHRIMP (Pankhurst et al., 2006); (2) Ordovician intrusive magmatic units located towards the south, in the Deseado Massif: e.g., Dos Hermanos Granite dated at ≥450 Ma and Ordovician granitic source of cobbles of Permian La Golondrina Conglomerate dated at ca. 475 Ma (U-Pb in zircons by SHRIMP; Pankhurst et al., 2003).

There are four metamorphic zircons with ages between 412 Ma (Lower Devonian, Lochkovian) and 318 Ma (Pennsylvanian/Mississippian boundary), including a pair at ca. 367 Ma (Upper Devonian, Famennian). All of these zircons could derive from coeval metamorphic sources present in the western Patagonian region. Metamorphic rocks of these ages form the metaigneous and metasedimentary basement of the Bariloche-Río Chico area. Amongst the published data for these basement rocks, conventional U-Pb zircon dating of the gneisses and migmatites of Collón Cura record an age of ca. 348 Ma (Varela et al., 2005), and zircon U-Pb SHRIMP dating of the El Maitén Gneiss record metamorphic overgrowths at 330, 340 and 365 Ma (Pankhurst et al., 2006). A conventional U-Pb zircon age of ca. 346 Ma obtained by Basei et al. (1999) for a foliated amphibolite from Cañadón de la Mosca was interpreted by these authors as reflecting the processes of magmatism, metamorphism and deformation occurred during the Upper Paleozoic. Upper Devonian metamorphic zircons may also derive from high-grade rocks of the Coastal Range of south-central Chile (e.g., Los Pabilos area), where they yielded a $^{40}Ar/^{39}Ar$ plateau age of ca. 361 Ma (Kato et al., 2008).

3.1.2.2. Sample CY334 (tonalitic orthogneiss). Twenty-three zircons were analyzed with ages ranging from Permian to Archean. Five analyses are clearly from xenocrystals with ages of 1862, 2408, 2627, 2666, and 2670 Ma (Fig. 6). However the age of 1862 Ma is considered as a minimum age because it represents discordant (35%) result. The remaining 18 analyses all provide Permian and slightly younger ages. Two of the three apparently younger results are highly discordant (74% and 381%, grains f.3-7 and f.8-1; larger ellipses of Fig. 5) and are not included in the pooled age. The third outlier analysis (grain f.6-1) has a significantly higher U-content than all other analyses (i.e. 614 ppm, compared to the average of 236 ppm), and it is also omitted on the basis of enhanced radiation damage and subsequent Pb-loss. Fifteen out of 18 analyses group at the $^{206}Pb/^{238}U$ age of 261.3 ± 2.7 Ma (1σ; MSWD = 0.049) (Fig. 5). This age is considered to be the age of crystallization of the tonalitic orthogneiss precursor.

Metamorphic conditions were not high enough to re-crystallize zircon, so the metamorphic age of this orthogneiss is not established. However, because the intrusion is considered to be syn-kinematic the age of metamorphism is interpreted to be indistinguishable from the magmatic age (late middle Permian, Capitanian). Field relationships also indicate that other metaigneous components of the Yaminué Complex, particularly those of leucogranitic composition, slightly postdate emplacement of the tonalitic orthogneiss precursor.

3.2. Hf isotopes

3.2.1. Methodology

Lu-Hf isotope analyses were carried out using a New Wave/Merchantek UP213 laser-ablation microprobe, attached to a Nu Plasma multi-collector ICP-MS at GEMOC (Geochemical Evolution and Metallogeny of Continents), Macquarie University, Sydney. Operating conditions include a beam diameter of ~55 μm, a 5 Hz repetition rate, with energy of ~0.4–0.8 mJ. Typical ablation times were 100–120 s, resulting in pits 40–60 μm deep. Mud Tank (MT) zircon was used as reference material which has an average $^{176}Lu/^{177}Hf$ ratio of 0.282522 ± 42 (2σ) (Griffin et al., 2007). MT analyzed in this study was within reported range (0.282514 ± 26; n = 2). More detail of the analytical techniques, precision and accuracy is described by Griffin et al. (2000, 2004).

Initial $^{176}Hf/^{177}Hf$ ratios are calculated using measured $^{176}Lu/^{177}Hf$ ratios, with a typical 2σ error uncertainty on a single analysis of $^{176}Lu/^{177}Hf$ ± (1%–2%). Such error reflects both analytical uncertainties and intragrain variation of Lu/Hf typically observed in zircons. Chondritic values of Scherer et al. (2001) (1.865×10^{-11}) have been used for the calculation of ε(Hf) values. Whilst a model of $(^{176}Hf/^{177}Hf)_i = 0.279718$ at 4.56 Ga and $^{176}Lu/^{177}Hf = 0.0384$ has been used to calculate model ages (T_{DM}) based on a depleted-mantle source, producing a present-day value of $^{176}Hf/^{177}Hf$ (0.28325) (Griffin et al., 2000, 2004). T_{DM} ages, which are calculated using measured $^{176}Hf/^{177}Hf$ of the zircon, give only the minimum age for the source material from which the zircon crystallized. We have therefore also calculated a "crustal" model age ($T_{DM(c)}$) for each zircon which assumes that the parental magma was produced from an average continental crust ($^{176}Lu/^{177}Hf = 0.015$) that was originally derived from depleted mantle. Data are presented in Table 2.

3.2.2. Results

3.2.2.1. Sample CY335a (biotite paraschist). Preliminary Hf isotope determinations have been carried out on two grains, dated at 447 ± 6 Ma (Ordovician, representative of the main source), and at 655 ± 11 Ma (Cryogenian–middle Neoproterozoic). The Ordovician and Cryogenian grains show $^{176}Hf/^{177}Hf$ ratios corresponding to ε(Hf) values of −0.32 and +0.48, with $T_{DM(c)}$ of 1543 Ma and 1624 Ma, respectively (Table 2). The ε(Hf) values close to zero of these zircons suggest that their primary sources contained small amounts of recycled crustal components (of Mesoproterozoic age; $T_{DM(c)}$ 1.56 Ga; Fig. 7).

3.2.2.2. Sample CY334 (tonalitic orthogneiss). Twelve measurements for Hf isotopes were undertaken on eight of the Permian zircons (population of 261 Ma) and on four inherited Neoarchean–Paleoproterozoic grains (Table 2). The Hf $T_{DM(c)}$ ages of Permian magmatic zircons are mainly Meso-Paleoarchean (2.97–3.35 Ga), with extremely low ε(Hf) values (up to −32.9 epsilon units), and Paleoproterozoic (1.92–2.1 Ga), with low ε(Hf) values (up to −13.0 epsilon units). The Hf $T_{DM(c)}$ ages of inherited Neoarchean zircons are also Meso-Paleoarchean (3.14–3.45 Ga), but more juvenile (ε(Hf) values between −0.3 and −4.5).

The Hf $T_{DM(c)}$ age of the younger inherited Paleoproterozoic zircon (1862 Ma; Orosirian) is Eoarchean (3.91 Ga), with an extremely low ε(Hf) value of −21.78, and that of the older inherited Paleoproterozoic zircon (2408 Ma; Siderian) is Paleoarchean, with a relatively more juvenile ε(Hf) value of −4.7.

These data (plotted on a $^{176}Hf/^{177}Hf$ vs. age diagram; Fig. 8) indicate that the Neoarchean–Paleoproterozoic crust underlying the Yaminué block, derived mostly from relatively juvenile Meso-Paleoarchean crust. Notably, the melts from which the Permian zircons crystallized, contained large amounts of Meso-Paleoarchean and/or Paleoproterozoic crust, reinforcing the indication of the occurrence of unexposed ancient crust in this area.

Table 2
Lu-Hf isotopes.

Spot	$^{238}Pb/^{206}Pb$ Ma	±	$^{207}Pb/^{206}Pb$ Ma	±	$^{176}Hf/^{177}Hf$	1σ	$^{176}Lu/^{177}Hf$	$^{176}Yb/^{177}Hf$	$^{176}Hf/^{177}Hf$ initial	ε(Hf)	1σ	T_{DM} (Ga)	$T_{DM(c)}$ (Ga)	Hf Chur (t)	Hf $_{DM}$ (t)
CY334, orthogneiss															
f.1-1	267	3			0.281679	0.000034	0.000644	0.01933	0.281676	−32.92	1.190	2.19	3.35	0.282606	0.283059
f.2-1	258	4			0.282336	0.000030	0.001154	0.03680	0.282330	−9.96	1.050	1.30	1.92	0.282612	0.283066
f.2.2	251	4			0.281836	0.000030	0.000812	0.02329	0.281832	−27.74	1.050	1.98	3.02	0.282616	0.283071
f.3-4			1873	17	0.280987	0.000031	0.000242	0.00691	0.280978	−21.78	1.085	3.09	3.91	0.281592	0.281886
f.3-6	269	4			0.281850	0.000023	0.000657	0.02027	0.281847	−26.83	0.805	1.95	2.97	0.282605	0.283058
f.4-1	258	4			0.281845	0.000017	0.000464	0.01412	0.281843	−27.21	0.595	1.95	2.99	0.282612	0.283066
f.4.2			2627	5	0.281138	0.000017	0.000827	0.02840	0.281096	−0.30	0.595	2.93	3.14	0.281105	0.281323
f.5-1			2670	17	0.280955	0.000020	0.000107	0.00375	0.280950	−4.53	0.700	3.12	3.45	0.281077	0.281290
f.6-1	245	3			0.282260	0.000014	0.000579	0.01929	0.282257	−12.83	0.490	1.39	2.09	0.282620	0.283075
f.6-2			2408	58	0.281123	0.000011	0.000171	0.00602	0.281115	−4.69	0.385	2.90	3.25	0.281247	0.281487
f.7-1	267	4			0.281848	0.000016	0.000564	0.01804	0.281845	−26.93	0.560	1.95	2.98	0.282606	0.283059
f.7-2	253	3			0.282257	0.000015	0.001893	0.06708	0.282248	−12.98	0.525	1.44	2.10	0.282615	0.283069
CY335, paraschist															
d.4-2	655	11			0.282348	0.000025	0.001168	0.04305	0.282332	0.48	0.875	1.28	1.62	0.282319	0.282726
d.8-2	447	5			0.282433	0.000021	0.001726	0.05975	0.282415	−0.32	0.735	1.18	1.54	0.282424	0.282848

^{176}Lu decay constant $= 1.865 \times 10^{-11}$(Scherer et al., 2001).

4. Key tectonic relationships of the Yaminué Complex

The aeromagnetic survey of the broader study region (Fig. 9a) has assisted the recognition the major structures. The Tardugno fault separates the easternmost component of the metaigneous unit of the Yaminué Complex, the Tardugno Granodiorite, from the Nahuel Niyeu Formation. It is coincident with the tectonic contact previously mapped on geological grounds (Caminos, 2001), although it can be traced for a much longer distance using the aeromagnetic data.

The aeromagnetic data were further modeled to gain additional structural/lithologic information usable for the overall geotectonic interpretation (Fig. 9e). The modeled transect (Fig. 9e) is based on the integration of two NW-oriented profiles extracted from the aeromagnetic survey data (see location, in Figs. 1 and 9a). To extend the geophysical interpretation where no aeromagnetic coverage is available, we have also used gravity data (Fig. 9b–d), leading us to recognize three crustal blocks, as discussed below.

4.1. Tardugno fault: recognition by aeromagnetics, and timing of activations

The regional extent identified for this structure suggests it is broadly coeval both with the thrusting that affects the Yaminué Complex itself, and with the nearby upthrust of the Nahuel Niyeu Formation over the Sierra Grande Formation (Chernicoff and Caminos, 1996b; von Gosen, 2003). The latest possible timing of this encompassing tectonic event is indicated by the late middle Permian (ca. 261 Ma) crystallization age of the syn-kinematic intrusion of the metaigneous unit of the Yaminué Complex (this article).

However, this can be a reactivation age, since time constraints from the exposed geology indicate a post-late Silurian–early Devonian (Sierra Grande Formation) and pre-early Permian (Navarrete Plutonic Complex: ca. 281 Ma) age for the Tardugno fault, possibly around the Mississippian–Pennsylvanian boundary, from here on also termed informally as middle Carboniferous, similarly as indicated by Chernicoff and Caminos (1996b) on the basis of the occurrence of (1) a depocenter of late Silurian–Devonian sediments (Sierra Grande Formation), aligned with and immediately east of the Tardugno fault, which we now see to stand out in the aeromagnetic map, as a partly discontinuous, NE trending magnetic low (see Fig. 9a), and (2) the "stitching" character of the Navarrete Plutonic Complex that intrudes the Tardugno fault. At this stage (i.e. middle Carboniferous), this roughly NE trending fault could have had a component of transcurrent motion in the context of the coeval, roughly NNW trending suture (i.e. oblique to the Tardugno fault) between the Southern Patagonia terrane and Patagonia terrane (*sensu stricto*) (see Sections 6 and 7, below).

A late middle Permian reactivation of the Tardugno fault would be indicated by the ca. 261 Ma crystallization age of the syn-kinematic intrusion of the metaigneous unit of the Yaminué Complex. During the late middle Permian, roughly S-directed thrusting along the Tardugno fault (second-order thrusts within the Yaminué Complex) would have been governed by the stress field associated with the accretion of the Patagonia composite terrane (e.g., von Gosen, 2003). In this context of reactivation, an intrusive contact between the Tardugno Granodiorite and the Nahuel Niyeu Formation (*cf.* von Gosen, 2003) would be permissive.

Additionally, it would also be possible that both the middle Carboniferous and the late middle Permian activations of the Tardugno fault pointed to reactivation ages, and that the Tardugno fault reflected a pre-existent terrane boundary suture (Fig. 9b), in agreement with isotopic and geochronologic data as summarized below.

(1) There exists a contrast between Nd model ages of the Paleozoic magmatic rocks exposed on either side of the suture, often supported by contrasting/different inheritance in either block, that is compatible with a tectonic boundary between two pre-Neoproterozoic crustal blocks. Particularly, as it will be seen below (see Sections 5 and 6, below), the Archean inheritance in the metaigneous unit of the Yaminué Complex points to the presence of a distinct basement to the west of the Tardugno fault.
(2) The predominance of Ordovician detrital zircons sourced from the Eastern Block (see Section 5, below), i.e. east of the Tardugno fault, in the precursor basin of the metasedimentary unit of the Yaminué Complex, located to the west of the Tardugno fault, indicate that the crustal blocks on either side were already juxtaposed by early Ordovician times. In the Section 7 (Tectonic evolution), below, we will refer to the precursor structure of the Tardugno fault, as the Tardugno suture, and constrain its possible timing to the late Neoproterozoic (Brazilian-age).

4.1.1. Other regional geophysical features

Other salient features in the aeromagnetic map are, e.g.: (1) Roughly NE trending fabric of the eastern part of the survey, reflecting the inner structural fabric of the Nahuel Niyeu Formation, e.g. schistosity planes and, possibly, unmapped thrust sheets like that exposed at the type area (Nahuel Niyeu stream); this trend is followed by Lower and Upper Paleozoic NE-elongated intrusions; the intrusive rocks of Lower Paleozoic age tend to produce lower magnetic intensities than the Upper Paleozoic intrusive rocks. The eastern third of the survey averages a higher magnetic intensity governed by deep sources i.e. inferred underlying occurrence of late Mesoproterozoic and "Ross-age" basement (see Section 6, below). In the southeastern corner of the survey, a subcircular feature could arise from a concealed eruptive center of the Jurassic Marifil volcanic rocks; (2) In the central-western part of the survey roughly NE trending lineaments arise from unmapped faults/fractures.

5. Crustal blocks

Modeling of the gravity data has allowed to recognize three unexposed crustal units, supported by geological, geochronological and isotopic (Nd, Hf) data that are analyzed in this section.

We use the term "crustal block" as a block of crust with an individual geological history that differs from the surrounding areas. Accordingly, we distinguish three blocks in the broader study region. As it will be seen below, two of these blocks are, in turn, interpreted as forming part of larger terranes defined by previous work.

5.1. Western block

It coincides with the northern portion of the Southern Patagonia terrane (cf. Ramos, 2010), and it is characterized by a broad positive Bouguer anomaly, the calculated density values reaching 2.75 g cm^{-3}. In accordance with the available Nd model ages, and inherited zircons in the exposed Paleozoic magmatic units (see Table 3), a predominant early Mesoproterozoic (ca. 1400–1600 Ma) to minor late Paleoproterozoic (1765–1811 Ma) reworked crust is predominant in this block, in addition to a less abundant and more juvenile early Neoproterozoic (Tonian) to late Mesoproterozoic (881–1084 Ma) crust. It has recently been argued that the latter tract of juvenile crust might pertain to a thinned crustal segment possibly associated with the early stage of Rodinia's break-up (Chernicoff et al., 2011).

Table 3
Hf model age and inherited zircons of the metaigneous unit of the Yaminué Complex, and Nd model ages and inherited zircons in the Paleozoic magmatic units exposed in the area and surroundings.

Tectonic blocks	Unit	T_{DM} (Nd and Hf)	Inheritance	
Western block	Piedra del Aguila Granite, earliest Permian		Statherian (1811 Ma) and Tonian (881 Ma)	1
	La Potranca (Los Altares, Chubut) granitoid, Permian	T_{DM} (Nd) 1765 Ma		1
	Comallo Granite, Permian	T_{DM} (Nd) 1600 Ma		2
	Cáceres (Gastre) Granite, Devonian	T_{DM} (Nd) 1521 Ma		1
	Paso del Sapo Granodiorite, Pennsylvanian	T_{DM} (Nd) 1514 Ma		1
	Pichiñanes Granite, late Mississippian	T_{DM} (Nd) 1485 Ma		1
	Rio Chico Tonalite, earliest Permian	T_{DM} (Nd) 1483 Ma		1
	Mamil Choique Granodiorite, early Permian	T_{DM} (Nd) 1418 Ma	Stenian (1031 Ma) and Cryogenian (745 Ma)	1
	Laguna del Toro (Gastre) Granodiorite, early Permian	T_{DM} (Nd) 1362 Ma	Tonian (966 Ma)	1
	Cañadón Mosca Granite, Mississippian	T_{DM} (Nd) 1084 Ma		1
	Cordón Serrucho Granite, Mississipian	T_{DM} (Nd) 996 Ma		1
	Platero Tonalite, Mississippian	T_{DM} (Nd) 884 Ma		1
	Colán Conué Granite, Devonian		Ordovicician, late Ross-age (476 Ma)	1
La Esperanza-Yaminué block	Metaigneous unit of the Yaminué Complex (late middle Permian tonalitic orthogneiss)	T_{DM} (Hf) Permian zircons: Meso-Paleoarchean (2.97–3.35 Ga; ε(Hf) −33). T_{DM} (Hf) Neoarchean inheritance: Meso-Paleoarchean (3.14–3.45 Ga; ε(Hf) −0.3). (**)	Neoarchean (2627 Ma, 2666 Ma, 2670 Ma) Paleoproterozoic (1873 Ma, 2408 Ma)	3
	Calvo–La Esperanza granites, early Triassic	T_{DM} (Nd) 1630 Ma		1
	La Esperanza Rhyolite, Permian	T_{DM} (Nd) 1516 Ma		1
	Prieto Granodiorite–La Esperanza Granodiorite, Permian	T_{DM} (Nd) 1448 Ma		1
	Lolog Granite, Devonian	T_{DM} (Nd) 1287 Ma	Brazilian-age (650 Ma); Ordovician (late Ross-age) (444 Ma)	1
	San Martín Granodiorite, Permian	T_{DM} (Nd) 1476 Ma	Stenian (1086 Ma) + Brazilian-age (621–636 Ma) and Ross-age (515–544 Ma)	1
Eastern block	Arroyo Salado Granite, Ordovician	T_{DM} (Nd) 1440 Ma	Stenian (1011 Ma) and Ross-age (531–572 Ma)	1
	Boca de la Zanja (Gaiman) Granodiorite, late Permian	T_{DM} (Nd) 1441 Ma	Stenian (1034 Ma) and Ross-age (511 Ma)	1
	Sierra Grande Granite, Ordovician	T_{DM} (Nd) 1432 Ma	Ross-age (503–506 Ma)	1
	Playas doradas/Punta Bahia Granite, Ordovician	T_{DM} (Nd) 1412 Ma	Stenian (1059 Ma); Brazilian-age (668 Ma)	1
	Navarrete Granodiorite, Permian	T_{DM} (Nd) 1233 Ma	Stenian (1048–1183 Ma) + Brazilian-age (636 Ma) and Ross-age (514 Ma). Also: Ordovician–early Silurian (late Ross-age): 462–431 Ma	1

(1) Pankhurst et al. (2006); (2) Varela et al. (2005); (3) this article. (**): see additional data in Table 1 and in text.

5.2. La Esperanza-Yaminué block

It is located within the central North Patagonian Massif. The origin of this block is referred to in the Discussion (Section 6, below).

On the whole, the western part of this block shows lower Bouguer anomaly values than the eastern part, possibly reflecting the abundant Permo-Triassic magmatism. In accordance with the available Nd model ages of the exposed Paleozoic magmatic units (Table 3), a reworked early Mesoproterozoic (ca. 1400–1600 Ma) crust is predominant in the western part of this block.

Distinctive geophysical and isotopic features characterize the most eastern portion of this block –that could be referred to as the Yaminué sub-block, as summarized below.

(1) The aeromagnetic data show higher intensity values (particularly, its northern portion) visible in the gridded data (Fig. 9a), and it also occurs a local increment in the Bouguer anomaly values; a gravity transect of Lince Klinger et al. (2010) carried out in this sector also picked out a higher gravity field over the Yaminué sub-block, and attributed it to deep sources.
(2) The conspicuous inheritance of Archean (plus Paleoproterozoic) zircons in the late middle Permian metaigneous unit of the Yaminué Complex (see Section 3, above), some of them with a clear core-rim relationship (Fig. 6), may indicate that this sub-block represents part of the older (Archean to Paleoproterozoic) nucleus of this crustal block. The latter would be underlain by denser (ca. 2.8 g cm^{-3}) lower crustal material pertaining to the Eastern block, wedged beneath the most eastern portion of the La Esperanza-Yaminué block; this interpretation is depicted in Fig. 9d. It should be noted that even if the Archean–Paleoproterozoic basement was uplifted to shallower levels at the eastern portion of the La Esperanza-Yaminué block, its density (ca. 2.6 g cm^{-3}) would not fit the residual Bouguer anomaly profile (Fig. 9d).

5.3. Eastern block

It corresponds to the Valcheta-Mina Gonzalito area of the Patagonia terrane (*sensu stricto*). The Eastern block extends to the east of the tectonic boundary between the Yaminué Complex (*cum* Tardugno Granodiotite) and the Nahuel Niyeu Formation. It is characterized by a broad Bouguer positive anomaly, with increasing values towards the east (Atlantic coastline) (Fig. 9d; the calculated density value for the suggested Mesoproterozoic crust and Ross-age magmatism is ca. 2.68 g cm^{-3}).

Mostly in accordance with the consistent ages of inherited zircons in the exposed Paleozoic magmatic units (see Table 3), it is possible to envisage that late Mesoproterozoic (1000–1100 Ma), late Neoproterozoic (i.e. Brazilian or Panafrican age; 620–660 Ma) and Ross-age (515–572 Ma; see Section 6) rocks may form part of this crustal block. Accordingly, the geotectonic model of Fig. 9d depicts (mostly) Ross-age magmatism intruding (mostly) late Mesoproterozoic basement. In addition, the available Nd model ages from the exposed Paleozoic magmatic units (Table 3) would also indicate the occurrence of reworked early Mesoproterozoic (ca. 1400–1600 Ma) crust.

6. Discussion

6.1. Isotopic and inheritance data supporting the block boundaries

In addition to the regional geophysical data referred to in Sections 4 and 5, the Nd- (and Hf; this article) isotope determinations in magmatic units, as well as the occurrence of old inherited zircons in such units, used in support of the proposed tectonic terrane boundaries in the analyzed region, are succinctly listed in Table 3.

As mentioned before, from a more regional perspective, the Western block referred to in this article forms part of the Southern Patagonia terrane (*cf.* Ramos, 2010). For this terrane, in addition to the data provided in Table 3, the meaningful occurrence of euhedral, inherited Paleoproterozoic to Archean magmatic zircons (between 1.96 and 3.41 Ga; Rolando et al., 2002) in the Mesozoic Patagonian Batolith has led the latter authors to infer the presence of Archean crust, partly assimilated by this Mesozoic magmatic arc, in this area. This evidence would be consistent with the occurrence of Archean detrital zircons of magmatic origin reported from the Cushamen Formation (Lizuain and Silva Nieto, 2002), more towards the north, suggesting that during the late Devonian–Carboniferous (?) depositional age of this unit, there was Archean basement exposed to denudation. It is interpreted that this ancient cratonic nucleus was largely consumed by the Pacific subduction and/or disrupted by the Phanerozoic intrusions.

On the other hand, the Eastern block pertains to the northern sector of the Patagonia terrane *sensu stricto* (*cf.* Ramos, 2010) that extends up to the eastern border of Tierra del Fuego, encompassing the basement of the eastern Deseado Massiff. Late Mesoproterozoic Nd model ages from the latter basement (1.05–1.32 Ga; Zappettini and Chernicoff, 2011, and references therein) add to the data presented in Table 3.

6.2. The identified terranes in a global geotectonic context

6.2.1. Patagonia terrane (sensu stricto)

It is worth noting that what is herein referred to as the Patagonia terrane (*sensu stricto*; *cf.* Ramos, 2010), is often geographically termed in literature as “Eastern Patagonia” (or “Patagonia Oriental”, in Spanish). Outstanding isotopic evidence from both SHRIMP geochronology and mostly Nd model ages indicate that the Patagonia terrane (*sensu stricto*) formed part of the Kalahari craton during the Mesoproterozoic. Evidence supporting such link includes the well known relationship between the Kalahari craton and the Malvinas/Falklands Plateau, and its eastern continuation, the Maurice-Ewing basement, both of which would have pertained to the same crustal fragment together with the Deseado Massif. Grenville-age juvenile island arc would have extended from southern Africa through the Malvinas/Falkland region, and into East Antarctica (Wareham et al., 1998; Thomas et al., 2000). The Mesoproterozoic age of the Cape Meredith Complex exposed at Cabo Belgrano (Thomas et al., 2000) is consistent with Mesoproterozoic inheritance and Nd model ages of the unexposed basement of the Deseado Massif (e.g., Zappettini and Chernicoff, 2011, and references therein), i.e. inherited zircons dated between 1.05 and 1.32 Ga, and Nd model ages ranging between 1.05 and 1.2 Ga, with ε(Nd) values between −0.5 and −2.43. The conspicuous middle Jurassic rhyolitic volcanism of Patagonia has been largely attributed to anatexis of Mesoproterozoic lower crust (Riley et al., 2001). The presence of a Mesoproterozoic basement in the Deseado Massif has also been suggested by Schilling et al. (2008), who also assigned the Deseado Massif and the Malvinas/Falklands Plateau to the same tectonic plate, providing geophysical evidence (Schilling and Tassara, 2008).

The Malvinas/Falkland Plateau may have lain adjacent to the eastern coast of southern Africa before the start of break-up of Gondwana in the Jurassic (e.g., Martin, 1986; Lawver and Scotese, 1987; McKerrow et al., 1992), although some authors (e.g., Mitchell et al., 1986; Taylor and Shaw, 1989; Marshall, 1994a, b) have suggested that the Malvinas/Falkland Islands micro-plate

would have rotated clockwise through up to 180° during the formation of the present continental configuration, 120° of which occurring during the early stages of the rifting of Gondwana, the remaining 60° occurring during the opening of the South Atlantic.

Kimbell and Richards (2008) and Richards et al. (1996), amongst others, have indicated that the onshore evidence for such rotations is not supported by the sedimentary sequences imaged in the offshore area, where there are no signs of disturbance of seismic reflectors that could be attributed to such lithospheric rotations. Therefore, this group of authors prefers the Malvinas/Falklands Plateau to be a fixed, rigid plate, translated to its present position without micro-plate rotation; they envisaged that the Malvinas/Falklands Islands started somewhere further southeast off the coast of South Africa than do workers who prefer the rotational model.

In regards of the Maurice-Ewing Bank, evidence for its continental nature, i.e. Mesoproterozoic gneisses and granitoids dated roughly at 1.1 Ga, is direct, as this basement has been drilled at DSDP Site 330 (Kimbell and Richards, 2008). Magnetic anomalies associated with the Maurice-Ewing Bank are consistent with the Mesoproterozoic basement and igneous bodies associated with later magmatism (Kimbell and Richards, 2008). Basement magnetic sources in southern Africa (e.g., Beattie Anomaly) and Antarctica may have originally been linked through the Malvinas/Falkland Plateau-Maurice-Ewing Bank (Jokat et al., 2003; Kimbell and Richards, 2008).

6.2.2. La Esperanza-Yaminué block

Isotopic evidence indicates that the La Esperanza-Yaminué block includes an unexposed Archean nucleus at present juxtaposed with the Mesoproterozoic basement of Patagonia (i.e. Patagonia terrane, *sensu stricto*, see previous section) along a first-order structure re-activated several times; the latter structure is interpreted as a suture between the La Esperanza-Yaminué block and Patagonia terrane *sensu stricto* (see Section 7, Tectonic evolution, below).

The isotopic data herein obtained for the metaigneous unit of the Yaminué Complex, particularly inheritance and Hf model ages, would suggest that the La Esperanza-Yaminué block represents a tectono-stratigraphic terrane originally unrelated to Patagonia-Kalahari, its adscription still requiring further isotopic data.

However, the inherited Neoarchean zircon cores identified in the late middle Permian zircons crystallized from the metaigneous unit of the Yaminué Complex, point to the occurrence of unexposed ancient crust in this area, comparable in age with the Neoarchean metaigneous rocks exposed in the eastern sector of the Río de la Plata craton (Nico Perez terrane; see e.g., Hartmann et al., 1999; Bossi et al., 2001; Santos et al., 2003), hence suggesting an affinity of the La Esperanza-Yaminué block with the Río de la Plata craton (see also Section 7, Tectonic evolution, below).

6.2.3. Southern Patagonia terrane

We use the term "Southern Patagonia terrane", as in Ramos (2010). The Southern Patagonia terrane lies west of the Patagonia terrane (*sensu stricto*), and it is separated from the latter by a north-northwest trending belt of late Devonian–early Carboniferous arc-type magmatic rocks, with superimposed middle Carboniferous metamorphism (Pankhurst et al., 2006). This igneous-metamorphic belt is thought to be related to the middle Carboniferous accretion of Southern Patagonia terrane (Ramos, 2008, 2010).

At least part of the Southern Patagonia terrane is bound to be underlain by Archean to Paleoproterozoic crust, as inferred by the identification of inherited idiomorphic magmatic zircons dated at 3.41–1.96 Ga in the Mesozoic igneous rocks of the Patagonian Cordillera, assigned to the partial assimilation of such crust (Rolando et al., 2002).

In this tectonic scenario, the middle Carboniferous accretion of a terrane with Archean–Paleoproterozoic crust –Southern Patagonia– to the western margin of Gondwana would point to its allochthonous nature. In regards of the origin of this terrane, the age of its crust is permissive of a Laurentian origin, since Archean crust of ca. 3.41 Ga and Paleoproterozoic crust of ca. 1.96 Ga are comparable in age with those of: (1) the Wopmay Orogen of ca. 1.9 Ga, that also contains basement rocks from the Archean Slave craton (>3 Ga) in its eastern region (e.g., Hildebrand et al., 2010), and (2) the Wyoming craton, that preserves rocks of 3.0–3.6 Ga (Chamberlain et al., 2003).

This origin would be consistent with the position of western Laurentia juxtaposed with East Antarctica-Australia prior to the break-up of Rodinia (Fig. 10), as indicated by Goodge et al. (2004), Hanson et al. (2004), Dalziel (2010) and Loewy et al. (2011). It would also be consistent with the "proto-SWEAT" connection between Australia and Laurentia proposed by Payne et al. (2009), valid between ca. 1740 and 1590 Ma (and likely at immediately earlier and later times).

Payne et al. (2009) have emphasized the possible correlation between the >3.1 Ga magmatic lithologies from the Slave craton and the Miller Range, envisaging the latter crustal block, part of the Mawson craton, in East Antarctica, as an orphaned fragment of Laurentia possibly derived from the Slave craton. Precisely, the position we envisage for the Southern Patagonia terrane before its separation from western Laurentia is somewhere in between the Slave Craton and the Miller Range crustal block. From this position, the Southern Patagonia terrane would have been detached as early as coevally with the actual detachment of Laurentia from East Antarctica-Australia during the early Neoproterozoic opening of the Pacific Ocean basin (and concomitant break-up of Rodinia). This being the case, the Southern Patagonia terrane would have drifted independently from Laurentia since the early Neoproterozoic, not serving as a tectonic tracer of the position of Laurentia at middle Carboniferous times.

7. Tectonic evolution

The new isotopic data of the Yaminué Complex presented in this article have been interpreted in conjunction with the isotopic data pertaining to a number of units exposed both in the nearby and in the broader study region. All in all, this has allowed to gain indirect information regarding the nature of the basements involved in the Patagonian region, and to reconstruct their diverse tectonic histories, in the context of the evolution of southern Gondwana and its early connection with Laurentia. Starting at early Neoproterozoic times, what follows is a concise account of the key stages of this evolution (Fig. 11).

7.1. Early Neoproterozoic (Tonian, ca. 1000–850 Ma)

On a global scale, during this period it is thought to have largely occurred the break-up of Rodinia. We assign the separation of the La Esperanza-Yaminué block from the Río de la Plata craton, as well as the detachment of the Southern Patagonia terrane from Laurentia, as part of this global event. The presence of juvenile Tonian inheritance (e.g., zircons dated at 881, 884, 996 Ma; Table 3) in some Paleozoic igneous units may point to the occurrence of early extensional magmatism in the unexposed basement of the Southern Patagonia terrane.

Otherwise, during this period there is no evidence of separation of the Patagonia terrane (*sensu stricto*) from the Kalahari craton.

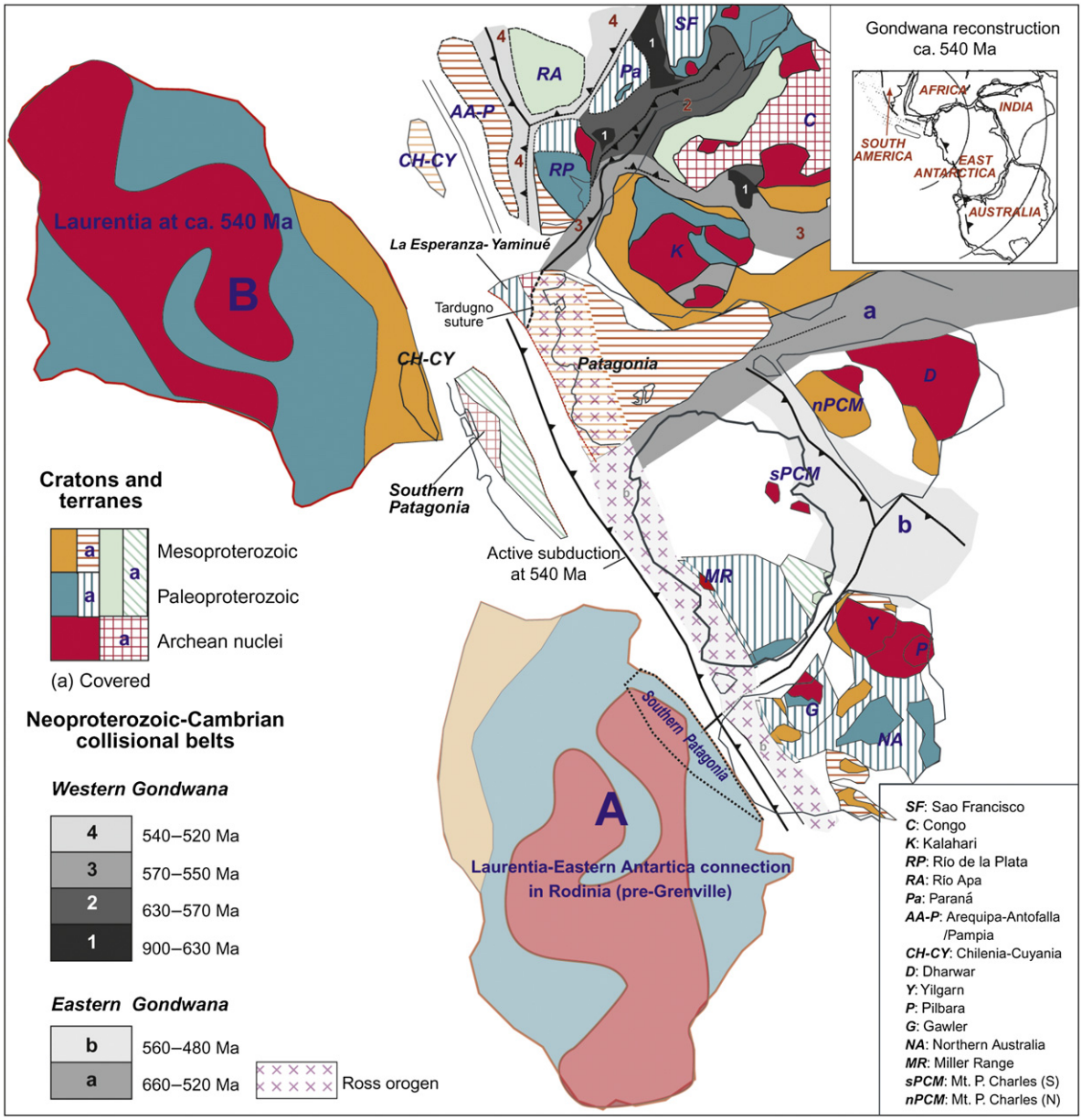

Figure 10. Reconstruction of Gondwana at ca. 540 Ma. (A): Reference position of Laurentia next to East Antarctica-Australia prior to the break-up of Rodinia (based on Goodge et al., 2004; Hanson et al., 2004; Payne et al., 2009; Dalziel, 2010). (B): Position of Laurentia juxtaposed with the newly assembled Gondwana at ca. 540 Ma (based on Dalziel, 2010). Precambrian provinces of Laurentia simplified from Goodge et al. (2004).

7.2. Late Neoproterozoic (late Cryogenian–early Ediacaran, ca. 660–620 Ma)

During this period it would have occurred the accretion of the La Esperanza-Yaminué block to the northwestern margin (present-day coordinates) of the Patagonia terrane (*sensu stricto*), along the Tardugno suture, as from this stage, the Patagonia terrane (*sensu stricto*) also includes the La Esperanza-Yaminué block. This collision would precede that occurred between the Río de la Plata and Kalahari cratons.

There is isotopic evidence of the occurrence of unexposed "eo-Brazilian" age (660–620 Ma) crust, possibly indicating the presence of unexposed remnants of an orogen of this age range. Evidence includes e.g. inherited zircons dated at ca. 650 Ma in the Lolog Devonian granite, and dated at 626–631 Ma in the San Martín Permian granite (both in the La Esperanza-Yaminué block), and inherited zircons dated at 636 Ma in the Navarrete Permian granodiorite (in the Patagonia terrane-*sensu stricto*); see Table 3.

7.3. Lower Paleozoic (ca. 542–450 Ma)

A number of facts point to the geographic continuity of the Ross orogen, from East Antarctica-Australia to the Patagonia terrane (*sensu stricto*). These include the proposed correlation between the Ordovician Punta Sierra Plutonic Complex of the Patagonia terrane (*sensu stricto*) and the slightly older Granite Harbour intrusives of the Transantarctic mountains, as well as between their hosting units, i.e. the El Jagüelito Formation and the Byrd and Beardmore Groups, respectively (González et al., 2011b, and references therein). Particularly convincing has been the identification of Atdabanian-Botomian Archeocyaths with strong affinity with the Antarctica-Australia paleobiogeographic province in limestone

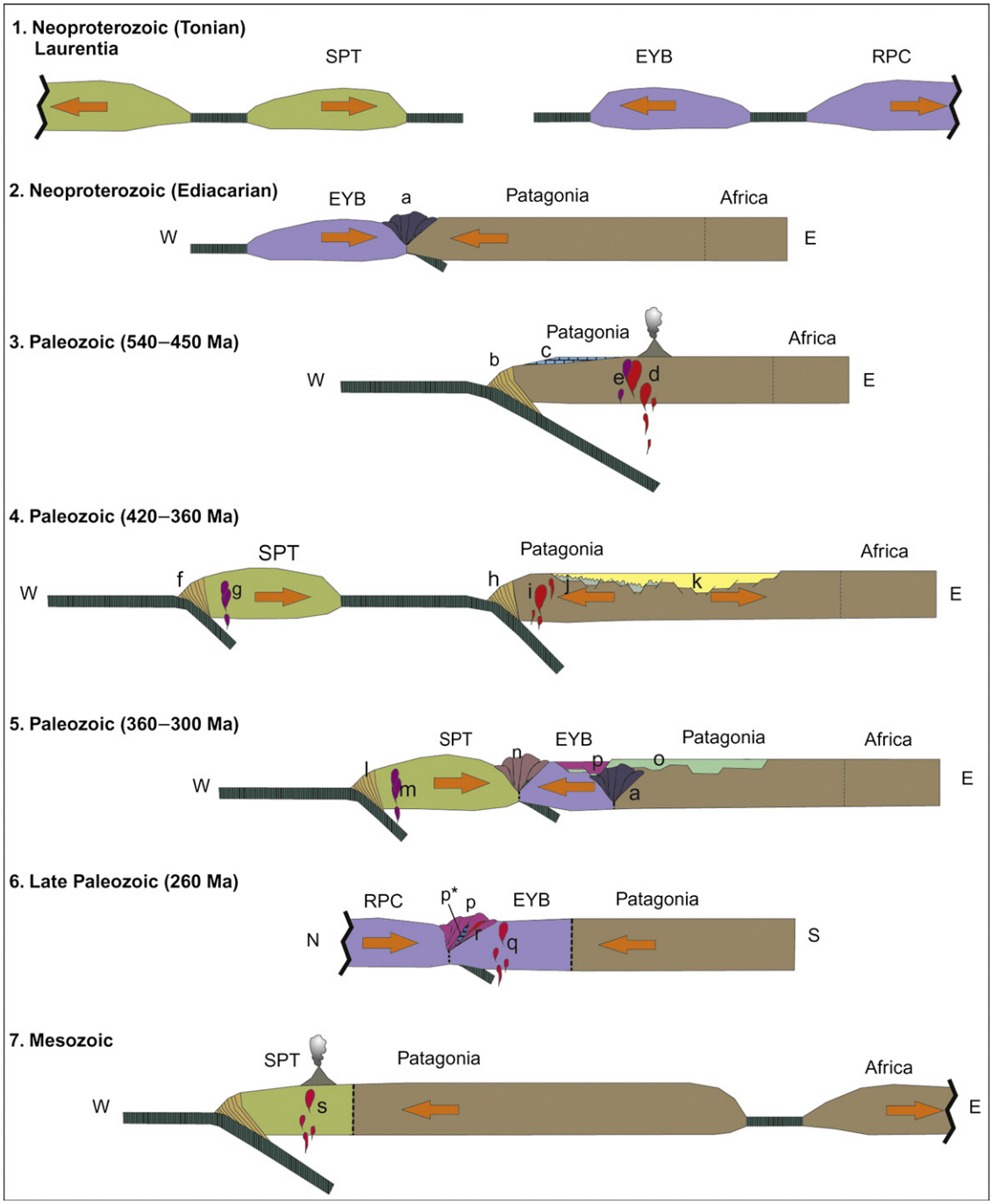

Figure 11. Tectonic evolution of the broader study region, from early Neoproterozoic to Mesozoic. References: a: Brazilian orogen, b: accretionary prism (Mina Gonzalito Gneiss), c: limestone platform, d: early Ross-age magmatism, e: Ordovician magmatism (e.g., Punta Sierra Plutonic Complex), f: accretionary prism, g: Devonian magmatism (western arc), h: accretionary prism, i: Devonian-Mississipian arc granitoids (eastern arc), j: Nahuel Niyeu and Coli Niyeu formations, k: Sierra Grande Formation, l: accretionary prism (western series), m: magmatic arc (Carboniferous; Chile), n: collisional belt (middle Carboniferous metamorphism), o: j + k (undifferentiated Nahuel Niyeu and Sierra Grande formations), p: metasedimentary unit of the Yaminué Complex (accretionary prism; *: slivers of marble), q: Permian north Patagonian arc, r: metaigneous unit of the Yaminué Complex (late middle Permian syncollisional granites), s: Andean-type magmatism. Acronyms: SPT: Southern Patagonia terrane, EYB: La Esperanza-Yaminué block, RPC: Río de la Plata craton. Note: for stage 6 (Late Paleozoic), transect is N-S; for the rest of stages, transects are E-W.

clasts of a conglomerate pertaining to the El Jagüelito Formation (Gonzalez et al., 2011a, b).

Indications of the unexposed occurrence of Ross-age magmatism in the Patagonia terrane (*sensu stricto*) comes from inherited zircons of this age range in a number of units such as the Ordovician Arroyo Salado Granite (inheritance at 531–572 Ma), the Ordovician Sierra Grande Granite (inheritance at 502–506 Ma), the Permian Boca de la Zanja Granodiorite (inheritance at 511 Ma), the Permian Navarrete Granodiorite (inheritance at 514 Ma), etc.; see Table 3. Additional evidence of early Cambrian igneous rocks, dated at 527–536 Ma, comes from borehole cores through the basement of the Magallanes Basin, Tierra del Fuego (zircon U-Pb SHRIMP; Hervé et al., 2010). Furthermore, the youngest and predominant detrital zircon age peaks dated at ca. 535 Ma and 535–540 Ma yielded by

the El Jagüelito Formation and the Mina Gonzalito Gneiss, respectively, have been interpreted as resulting from erosion from a nearby, coeval and active magmatic arc (Pankhurst et al., 2006).

All in all, the evidence mentioned above would allow to extend the tectonic model envisaged by Goodge et al. (2004) for Eastern Antarctica, actually to the Patagonia terrane (*sensu stricto*) itself, encompassing a restricted platform at the active margin of Eastern Antarctica-Patagonia terrane (*sensu stricto*) in a forearc position, plus a magmatic arc, these being two key elements of the Ross orogen. The eastward dipping (present coordinates) subduction zone defined at the margin of Eastern Antarctica would have extended to the Patagonia terrane (*sensu stricto*) during the Ross calc-alkaline arc magmatism, running closely to the present-day coastline of the eastern Patagonian region, and terminating at the boundary with the La Esperanza-Yaminué block. In this framework, the Cambrian A-type Cape granites of southern Africa (e.g., Chemale et al., 2010, and references therein) would have developed in a backarc-intraplate context. Locally, sinorogenic anatectic granitoids developed during the Lower Ordovician (e.g., Valcheta Pluton; Gozalvez, 2009, and equivalent bodies in the Mina Gonzalito area; Giacosa, 1997). In this tectonic scheme, the sedimentary protolith of the Ordovician Mina Gonzalito Gneiss could represent remnants of the Cambrian accretionary prism developed at the western margin of the Patagonia terrane (*sensu stricto*), bearing prominent late Neoproterozoic–early Cambrian detritus from the Ross orogen.

7.4. Paleozoic (late Silurian–early Devonian, ca. 420–400 Ma)

By late Silurian–early Devonian times, the southern margin of Gondwana would have been a passive margin, with representative sedimentation being recorded at many present-day distant locations, e.g. Sierras Australes of Buenos Aires Province, Patagonia terrane (*sensu stricto*), Malvinas/Falkland Plateau, Cape Basin of South Africa and Ellsworth Mountains of Antarctica (e.g., Harrington, 1947; Goldstrand et al., 1994; Marshall, 1994b; de Wit et al., 2007; Ramos, 2008; Tankard et al., 2009; and references therein). Large-scale lithospheric extension would have occurred during this stage (e.g., Hunter and Lomas, 2003).

In the Patagonia terrane (*sensu stricto*), quartz-rich sediments were deposited (i.e. Sierra Grande Formation) overlying the Ross-age magmatic units (e.g., Punta Sierra Plutonic Complex). The age of the detrital zircons identified in the Sierra Grande Formation mostly show variable but prominent late Neoproterozoic, early Cambrian and early Ordovician peaks, as well as a less prominent late Mesoproterozoic population (Pankhurst et al., 2006; Uriz et al., 2010). Hence the late Silurian–early Devonian Sierra Grande Formation and the early Cambrian El Jaguelito Formation (see above) share the same main provenance, i.e. unexposed (early to late) Ross-age magmatic rocks, plus the country rocks thereof, i.e. largely late Mesoproterozoic basement.

During this period, a small ocean would have been developed between the Patagonia terrane (*sensu stricto*) and the Río de la Plata craton, i.e. roughly perpendicular to the coeval margin of southern Gondwana, possibly being initiated as a trough located at a re-entrant on the continental margin, narrowing inboard of it. This initial aulacogen stage would have been followed by short-lived rifting, with the formation of oceanic crust in a Red Sea-like context, analogous to that proposed for the early evolution of the Damara orogen (e.g., Miller, 1983). The roughly east-west trending (present-day coordinates) gravimetric and aeromagnetic high recorded at the northern boundary of the Patagonian region (Chernicoff and Zappettini, 2004) may partly account for the concealed remnants of rift-related magmatism that may have been preserved from consumption via south-dipping subduction in a later stage (see Permian stage, below). The location of the proposed basin coincides geographically (though not geochronologically or genetically) with the Colorado ocean of Rapalini et al. (2010).

Also during this time of extensional tectonics, the Tardugno suture (boundary between the Patagonia terrane (*sensu stricto*) and the La Esperanza-Yaminué block) would have been re-activated as a zone of transtensional faulting, with the late Silurian–Devonian sedimentary fill (Sierra Grande Formation) reaching this area, the farthest west (present-day coordinates) in the eastern Patagonian region.

7.5. Paleozoic (middle–late Devonian, ca. 400–360 Ma)

During this stage, eastward subduction would have initiated at the western margin of the Patagonia terrane (*sensu stricto*), giving rise to an Upper Devonian magmatic arc that traverses discontinuously a large part of the present-day Patagonian region, following a NNW trend. Representative exposures of this arc are e.g. granitoids exposed at the North-Patagonian Cordillera, dated at ca. 386–419 Ma (Varela et al., 2005), at 395–401 Ma (Pankhurst et al., 2006) and at 393 ± 3.3 Ma (Godoy et al., 2008), as well as tonalites exposed in the Deseado Massif (395 ± 4 Ma; Pankhurst et al., 2003). This magmatism would extend into the Mississippian (e.g., La Leona Granite, Deseado Massif, dated at 344 ± 4 Ma; Pankhurst et al., 2003).

Subduction would have been concomitant with the approach of the Southern Patagonia terrane towards the western margin of the Patagonia terrane (*sensu stricto*)/Gondwana, with which it would have collided in middle Carboniferous times as evidenced by coeval metamorphism (Pankhurst et al., 2006). The origin of the Southern Patagonia terrane has been discussed above (see Section 6, Discussion, above).

The existence of Devonian magmatic arc plutons, as evidenced e.g. by the Chaitén metatonalite of south-central Chile, dated at 387.9 ± 6.2 Ma (U-Pb LAM-ICP-MS method; Duhart et al., 2009) and granitic intrusive bodies also known to occur in the subsurface of the Depresión Central of Chile, where they have been dated at 359.3 ± 4.4 Ma (Ar/Ar in hornblende; Duhart et al., 2001), would indicate that the western margin of the Southern Patagonia terrane was also affected by east-dipping active subduction. In this context the presence of relict eclogite-amphibolite assemblages in the Coastal Range of south-central Chile (41 S) that yielded $^{40}Ar/^{39}Ar$ plateau age of 361 ± 1.7 Ma, and retrograded by Carboniferous times (ca. 325 Ma, $^{40}Ar/^{39}Ar$ plateau age) provide evidence of pre-Carboniferous high *p*-T metamorphism along the southwestern continental margin of Gondwana related to subduction of oceanic lithosphere, that would have began prior to 361 Ma (late Devonian) (Kato et al., 2008).

Detrital zircon from the Bahía Mansa Metamorphic Complex on the Main Chiloé Island, south-central Chile, of uppermost Devonian–Carboniferous age (360 Ma) could have derived from Devonian granites locally present in the subsurface of the Depresión Central of Chile (Duhart and Adriadola, 2008).

7.6. Paleozoic (Carboniferous, 360–300 Ma)

By middle Carboniferous times the Southern Patagonia terrane would have collided against the western margin of the Patagonia terrane (*sensu stricto*), causing the termination of the subduction-related magmatic arc, whose latest evidence of its occurrence is Mississippian (i.e. granitoids dated at ca. 323–330 Ma at Cordón del Serrucho and nearby areas; Varela et al., 2005; Pankhurst et al., 2006). The timing of the collisional event would be constrained by the emplacement of the peraluminous early Pennsylvanian

S-type leucogranites of Paso del Sapo and Sierra de Pichiñanes, dated at 314 ± 2 Ma and 318 ± 2 Ma, respectively (Pankhurst et al., 2006). The precise trace of the suture is not well defined, though it is bound to closely follow the NNW trend of the late Devonian Mississippian magmatic arc. Note that in contrast to the interpretation presented in this article, Pankhurst et al. (2006) considered that the colliding crustal fragment causing the middle Carboniferous metamorphism would have been the Deseado Massif, regarding it as parautochthonous (detached from southwestern Gondwana at Cambrian times, and re-accreted during the Carboniferous).

Meanwhile, east-dipping subduction continued at the western margin of the Southern Patagonia terrane, with the accumulation of a sedimentary sequence that would later be incorporated into the accretionary prism of the Coastal Range. Partly coevally, after ca. 318 Ma (youngest detrital zircon), the protolith of the metasedimentary unit of the Yaminué Complex may have been deposited in a more inboard position, as it received detritus both from the middle Carboniferous collisional belt and from Ross-age sources located in the Patagonia terrane (*sensu stricto*). This being the case, the protolith of the metasedimentary unit of the Yaminué Complex should be regarded as post-collisional with respect to the middle Carboniferous collisional event (see ulterior context of deformation of these sediments at middle Permian, below).

7.7. Paleozoic (Permian, 300–260 Ma)

At early Permian times, the spread in the narrow ocean developed between the Río de la Plata craton and the Patagonia composite terrane (see late Silurian–early Devonian stage, above) was reversed, with south-dipping subduction being initiated at the northern margin (present-day coordinates) of the Patagonia composite terrane.

Ultimately, this subduction lead to the collision between the Río de la Plata craton (lower plate) and the Patagonia composite terrane (upper plate), with the development of an associated collisional accretionary prism during the middle Permian, represented by (though possibly not limited to) the strongly deformed metasedimentary unit of the Yaminué Complex. In this context, the marbles of this unit may represent upthrust slivers of deformed passive margin limestones, tectonically imbricated with the predominantly siliciclastic metasedimentary rocks of the accretionary prism.

The deformation and metamorphism of the metasedimentary unit of the Yaminué Complex, under lower amphibolite facies, occurred about 50 Ma after the onset of its deposition, i.e. at ca. 261 Ma, coevally with the syn-kinematic intrusion of the metaigneous unit of the Yaminué Complex. This timing tends to confirm that in the northern Patagonian region it took place a strong deformational event independent of that occurred at middle Carboniferous times, which could be attributed to the collision of the Patagonia (composite terrane) against the Rio de la Plata craton (e.g., Ramos, 2008). A number of Permian granitoids identified in the northern Patagonian region would be partly syncollisional (e.g., Yaminué metaigneous unit) and partly pre-collisional (e.g., Navarrete Granodiorite, Prieto Granodiorite). The latter framework for the Permian magmatism is quite different to that proposed by Pankhurst et al. (2006), according to whom this magmatism would have been caused by a major access of heat to the crust following the slab break-off after the middle Carboniferous collision of the Deseado Massif. Notably, this latter option does not seem to explain the strong deformation occurred during the late middle Permian, as conspicuously portrayed by the Yaminué Complex.

Acknowledgments

This work received financial support from Research Grant PIP-11220090100181 (CONICET, Council for Scientific and Technical Research of Argentina) and SEGEMAR. The investigation forms part of the Geological Map 4166-9, Estación Muster Sheet, scale 1:100,000, of the Geological Survey of Argentina (SEGEMAR). SEGEMAR's permission to publish information contained in this map, as well as aeromagnetic data proprietary to SEGEMAR, is kindly acknowledged. Zircon grains were analyzed on the SHRIMP II operated by a Western Australia university–government consortium with Australia Research Council support. BSE (Back-Scattered Electrons) images were carried out using facilities at the CMCA (Centre for Microscopy, Characterization, and Analyses), which is supported by funding from UWA and the governments of Western Australia and Australia. Prof. Fernando Hongn and an anonymous reviewer helped improve an earlier version of the manuscript.

Appendix A

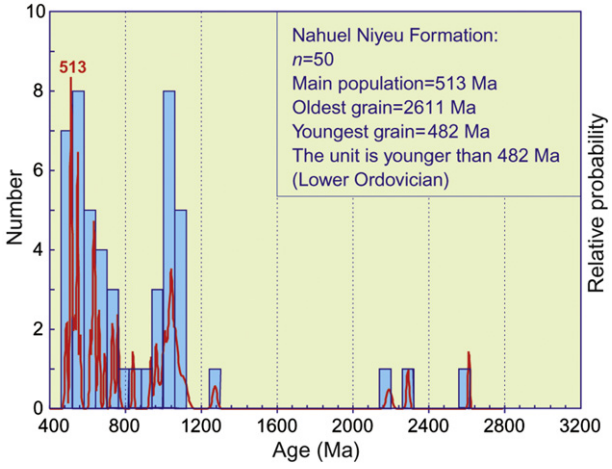

Figure A1. Probability plot based on the zircon U-Pb SHRIMP ages of the Nahuel Niyeu Formation provided by Pankhurst et al. (2006) as Supplementary Data. Re-plotting of these data yield new clues on the geological framework of the region.

References

Basei, M.A.S., Brito Neves, B.B., Varela, R., Teixeira, W., Siga Jr., O., Sato, A.M., Cingolani, C., 1999. Isotopic dating on the crystalline basement rocks of the Bariloche region, Río Negro, Argentina. II South American Symposium on Isotope Geology, Anales SEGEMAR 34, 15–18. Villa Carlos Paz, Córdoba.

Basei, M.A.S., Varela, R., Sato, A.M., Siga Jr., O., Llambías, E.J., 2002. Geocronología sobre rocas del Complejo Yaminué, Macizo Norpatagónico, Río Negro, Argentina. In: 15 Congreso Geológico Argentino, Calafate, Actas 3, 117–122.

Bjerg, E.A., Gregori, D.A., Labudía, C.H., 1997. Geología de la región de El Cuy, Macizo de Somuncura, Provincia de Río Negro, Argentina. Revista de la Asociación Geológica Argentina 52 (3), 387–399.

Bossi, J., Campal, N., Hartmann, L.A., Schipilov, A., 2001. Predevoniano en el Uruguay: terrenos y SHRIMP II. XI Congreso Latinoamericano y III Congreso Uruguayo de Geología, Digital Proceedings, No. 94.

Busteros, A., Giacosa, R., Lema, H., 1998. Hoja Geológica 4166-IV, Sierra Grande. Provincia de Río Negro. Instituto de Geología y Recursos Minerales, Servicio Geológico Minero Argentino, Buenos Aires, Boletín 241, 75 pp.

Caminos, R., 1983. Descripción geológica de las Hojas 39g, Cerro Tapiluke y 39h, Chipauquil, provincia de Río Negro. Servicio Geológico Nacional, 32 pp. (Unpublished Report).

Caminos, R., 2001. Hoja Geológica 4166-I Valcheta, provincia de Río Negro. In: Servicio Geológico Minero Argentino Boletín, vol. 310, Buenos Aires, 78 pp.

Caminos, R., Chernicoff, C., Varela, R., 1994. Evolución tectónico-metamórfica y edad del Complejo Yaminué, Basamento pre-andino Norpatagónico, República Argentina. In: 7 Congreso Geológico Chileno, Concepción, Actas II, pp. 1301–1305.

Chamberlain, K.R., Frost, C.D., Ronald Frost, B., 2003. Early Archean to Mesoproterozoic evolution of the Wyoming Province: Archean origins to modern

lithospheric architecture. Canadian Journal of Earth Sciences 40 (10), 1357–1374.
Chemale Jr., F., Scheepers, R., Gresse, P.G., Van Schmus, W.R., 2010. Geochronology and sources of late Neoproterozoic to Cambrian granites of the Saldania Belt. International Journal of Earth Sciences. http://dx.doi.org/10.1007/s00531-010-0579-1.
Chernicoff, C.J., 1994. Estructura del basamento cristalino del área Yaminué-Nahuel Niyeu, Macizo Nordpatagónico. Thesis Doctoral. Facultad de Ciencias Exactas y Naturales, Universidad de Buenos Aires. 165 pp. (Unpubl.).
Chernicoff, C.J., Caminos, R., 1996a. Estructura y metamorfismo del Complejo Yaminué, Macizo Nordpatagónico, Provincia de Río Negro. Revista de la Asociación Geológica Argentina 51 (2), 107–118.
Chernicoff, C.J., Caminos, R., 1996b. Estructura y relaciones estratigráficas de la Formación Nahuel Niyeu, sector nororiental del Macizo Nordpatagónico, Provincia de Río Negro. Revista de la Asociación Geológica Argentina 51 (3), 201–212.
Chernicoff, C.J., Gozalvez, M.R., 2012. Mapa Geológico 4166-9 Estación Muster, provincia de Río Negro. Escala 1:100.000. Servicio Geológico Minero Argentino, Buenos Aires.
Chernicoff, C.J., Zappettini, E., 2004. Geophysical evidence for terrane boundaries in south-central Argentina. Gondwana Research 7 (4), 1105–1116.
Chernicoff, C.J., Zappettini, E.O., Santos, J.O.S., Belousova, E., McNaughton, N.J., 2011. Hf isotope study of Paleozoic metaigneous rocks of La Pampa province, and implications for the occurrence of juvenile early Neoproterozoic (Tonian) magmatism in south-central Argentina. Journal of South American Earth Sciences 32 (4), 477–484.
Dalla Salda, L.H., Aragón, E., Benialgo, A., Pezzotti, C., 2003. Una plataforma calcárea en el Complejo Mina Gonzalito, provincia de Río Negro. Revista de la Asociación Geológica Argentina 58 (2), 209–217.
Dalziel, I.W.D., 2010. The North-West Highlands Memoir: A Century-old Legacy for Understanding Earth Before Pangaea. Geological Society, London, Special Publications 335, 189–205.
de Wit, M., Armstrong, R., Bowring, S., Alexander, J., Branch, T., Decker, J., Ghosh, J., Moore, S., Lindeque, A., Stankiewicz, J., Rakatolosofo, N., 2007. Chrono-, chemical-, seismic-, electrical- and tectono-stratigraphy across parts of the Cape Fold Belt – Karoo Basin of South Africa: new foundations for correlations across the South Atlantic. 1 Workshop – Problems in Western Gondwana Geology, Gramado. Extended Abstracts, 34–41.
Duhart, P., Adriadola, A., 2008. New time-constraints on provenance, metamorphism and exhumation of the Bahía Mansa Metamorphic Complex on the Main Chiloé Island, south-central Chile. Revista Geológica de Chile 35 (1), 79–104.
Duhart, P., Cardona, A., Valencia, V., Muñoz, J., Quiroz, D., Hervé, F., 2009. Evidencias de basamento Devónico, Chile centro-sur (41–44°S). XII Congreso Geológico Chileno. Santiago. Extended Abstract, S8_009.
Duhart, P., McDonough, M., Muñoz, J., Martin, M., Villeneuve, M., 2001. El Complejo Metamórfico Bahía Mansa en la Cordillera de la Costa del centro-sur de Chile (39°30′–42°00′S): geocronología K-Ar, Ar/Ar y U-Pb e implicancias en la evolución del margen sur-occidental de Gondwana. Revista Geológica de Chile 28 (2), 179–208.
Giacosa, R.E., 1997. Geología y petrología de las rocas pre-cretácicas de la región de sierra Pailemán, Provincia de Río Negro. Revista de la Asociación Geológica Argentina 52 (1), 65–80.
Godoy, E., Hervé, F., Fanning, M., 2008. Edades U-Pb SHRIMP en granitoides del Macizo Nordpatagónico: implicancias geotectónicas. In: 17 Congreso Geológico Argentino, San Salvador de Jujuy, Actas II, pp. 1288–1289.
Goldstrand, P.M., Fitzgerald, P.G., Redfield, T.F., Stump, E., Hobbs, C., 1994. Stratigraphic evidence for the Ross Orogeny in the Ellsworth Mountains. Implications for the evolution of the paleo-margin of Gondwana. Geology 22, 427–430.
González, P.D., Poiré, P.G., Varela, R., 2002. Hallazgo de trazas fósiles en la Formación El Jagüelito y su relación con la edad de las metasedimentitas, Macizo Nordpatagónico Oriental, provincia de Río Negro. Revista de la Asociación Geológica Argentina 57, 35–44.
González, P.D., Sato, A.M., Llambías, E.J., Varela, R., 2008. Geología del corrimiento Piedras Coloradas, Basamento Ígneo-Metamórfico de Las Grutas, Río Negro. In: 17 Congreso Geológico Argentino, San Salvador de Jujuy, Actas II, pp. 845–846.
González, P.D., Sato, A.M., Naipauer, M., Varela, R., Llambías, E.J., Basei, M.A.S., 2011b. Does Patagonia represent a missing piece detached from the Ross Orogen? Gondwana 14. Abstracts.
González, P.D., Tortello, M.F., Damborenea, S.E., 2011a. Early Cambrian archaeocyathan limestone blocks in low-grade meta-conglomerate from El Jagüelito Formation (Sierra Grande, Río Negro, Argentina). Geologica Acta 9, 1–1 4.
Goodge, J., Williams, I., Myrow, P., 2004. Provenance of Neoproterozoic and coger Paleozoic siliciclastic rocks of the central Ross origin, Antarctica: detrital record of rift-, passive-, and active-margin sedimentation. Geological Society of America Bulletin 116 (9/10), 1253–1279.
Gozalvez, M.R., 2009. Petrografía y edad $^{40}Ar/^{39}Ar$ de leucogranitos peraluminosos al oeste de Valcheta. Macizo Nordpatagónico (Río Negro). Revista de la Asociación Geológica Argentina 64 (2), 285–294.
Griffin, W.L., Belousova, E.A., Shee, S.R., Pearson, N.J., O'Reilly, S.Y., 2004. Archean crustal evolution in the northern Yilgarn Craton: U-Pb and Hf-isotope evidence from detrital zircons. Precambrian Research 131, 231–282.
Griffin, W.L., Pearson, N.J., Belousova, E.A., Jackson, S.R., van Achterbergh, E., O'Reilly, S.Y., Shee, S.R., 2000. The Hf isotope composition of cratonic mantle: LAM-MC-ICPMS analysis of zircon megacrysts in kimberlites. Geochimica et Cosmochimica Acta 64, 133–147.
Griffin, W.L., Pearson, N.J., Belousova, E.A., Saeed, A., 2007. Reply to "Comment to short-communication 'Comment: Hf-isotope heterogeneity in zircon 91500' by W.L. Griffin, N.J. Pearson, E.A. Belousova and A. Saeed (Chemical Geology 233 (2006) 358–363)" by F. Corfu. Chemical Geology 244, 354–356.
Hanson, R.E., Crowley, J.L., Bowering, S.A., Ramezani, J., Gose, W.A., Siedel, E.K., Blenkinsop, T.G., Mukwakwami, J., 2004. Coeval Large-Scale Magmatism in the Kalahari and Laurentian Cratons during Rodina Assembly. Science 304, 1126–1129.
Harrington, H.J., 1947. Explicación de las Hojas Geológicas 33m (Sierra de Curamalal) y 34m (Sierra La Ventana). Provincia de Buenos Aires. Boletín de la Dirección de Minería y Geología, Buenos Aires, 61 pp.
Hartmann, L.A., Santos, J.O.S., 2004. Predominance of high Th/U, magmatic zircon in Brazilian Shield sandstones. Geology 32 (1), 73–76.
Hartmann, L.A., Santos, J.O.S., Leite, J.A.D., McNaughton, N.J., 1999. Deepest exposed crust of Brazil — SHRIMP establishes three events. Geology 27, 947–950.
Hervé, F., Fanning, C.M., Pankhurst, R.J., Mpodozis, C., Klepeis, K., Calderón, M., Thomson, S.N., 2010. Detrital zircon SHRIMP U-Pb age study of the Cordillera Darwin Metamorphic Complex of Tierra del Fuego: sedimentary sources and implications for the evolution of the Pacific margin of Gondwana. Journal of the Geological Society 167, 555–568.
Hildebrand, R.S., Hoffman, P.F., Bowring, S.A., 2010. The Calderian orogeny in Wopmay orogen (1.9 Ga), northwestern Canadian Shield. Geological Society of America Bulletin 122 (5–6), 794–814.
Hunter, M.A., Lomas, S.A., 2003. Reconstructing the Siluro-Devonian coastline of Gondwana: insights from the sedimentology of the Port Stephens Formation, Falkland Islands. Journal of the Geological Society 160, 459–476.
Jokat, W., Boebel, T., König, M., Meyer, U., 2003. Timing and geometry of early Gondwana breakup. Journal of Geophysical Research 108 (B9), 2428.
Kato, T.T., Sharp, W.D., Godoy, E., 2008. Inception of a Devonian subduction zone along the southwestern Gondwana margin: $^{40}Ar/^{39}Ar$ dating of eclogite–amphibolite assemblages in blueschist boulders from the Coastal Range of Chile (41°S). Canadian Journal of Earth Sciences 45, 337–351.
Kimbell, G.S., Richards, P.C., 2008. The three-dimensional lithospheric structure of the Falkland Plateau region based on gravity modelling. Journal of the Geological Society of London.
Lawver, L.A., Scotese, C.R., 1987. A revised reconstruction of Gondwanaland. In: McKenzie, G.D. (Ed.), Gondwana Six: Structure, Tectonics and Geophysics. AGU Geophysical Monographs, 40, pp. 17–23.
Loewy, S.L., Dalziel, I.W.D., Pisarevsky, S., Connelly, J.N., Tait, J., Hanson, R.E., Bullen, D., 2011. Coats Land crustal block, East Antarctica: a tectonic tracer for Laurentia? Geology 39 (9), 859–862.
Lince Klinger, F., Gimenez, M.E., Martinez, M.P., Rapalini, A., Novara, I., 2010. Poisson relation applied to the Navarrete Plutonic Complex, northeast North-Patagonian Massif, Argentina. Geofísica Internacional 49 (4), 263–274.
Lizuain, A., Silva Nieto, D., 2002. Observaciones geológicas en la región del Río Chico, Gastre, Río Chubut medio. Provincia del Chubut. XVI Congreso Geológico Argentino, Actas. La Plata.
López de Luchi, M.G., Rapalini, A.E., Tomezzoli, R.N., 2010. Magnetic Fabric and Microstructures of Late Paleozoic granitoids from the North Patagonian Massif: evidence of a collision between Patagonia and Gondwana? Tectonophysics 494 (1e2), 118–137.
López de Luchi, M.G., Wemmer, K., Rapalini, A.E., 2008. The cooling history of the North Patagonian Massif: first results for the granitoids of the Valcheta area, Río Negro, Argentina. VI South American Symposium on Isotope Geology, Digital Proceedings, Abstract. 33.
Ludwig, K.R., 2001. Squid 1.02: A Users Manual. Berkeley Geochronology Centre, Special Publication. 2, 19 pp.
Ludwig, K.R., 2003. Isoplot 3.00, A Geochronological Took-kit for Excel. Berkeley Geochronology Center, Special Publication 4, 67 pp.
Marshall, J.E.A., 1994a. The Falkland Islands and the early fragmentation of Gondwana: implications for hydrocarbon exploration in the Falkland Plateau. Marine and Petroleum Geology 11 (5), 631–636.
Marshall, J.E.A., 1994b. The Falkland Islands: a key element in Gondwana palaeogeography. Tectonics 13, 499–514.
Martin, A.K., 1986. Microplates in Antarctica. Nature 319, 100–101.
Martínez Dopico, C.I., López de Luchi, M.G., Rapalini, A.E., Kleinhanns, I.C., 2011. Crustal segments in the North Patagonian Massif, Patagonia: an integrated perspective based on Sm-Nd isotope systematics. Journal of South American Earth Sciences 31, 324–341.
McKerrow, W.S., Scotese, C.R., Brasier, M.D., 1992. Early Cambrian continental reconstructions. Journal of the Geological Society of London 149, 599–606.
Miller, R.McG., 1983. The Pan-African Damara Orogen of Southwest Africa/Namibia. In: Miller, R.Mc G. (Ed.), Evolution of the Damara Orogen. Special Publication of the Geological Society of South Africa, 11, pp. 431–515.
Mitchell, C., Taylor, G.K., Cox, K.G., Shaw, J., 1986. Are the Falkland Islands a rotated microplate? Nature 319, 131–134.
Naipauer, M., González, P.D., Varela, R., Sato, A.M., Chemale Jr., F., Llambías, E., Greco, G., 2011. Edades U-Pb (LA-ICP-MS) en circones detríticos del Miembro Polke, Formación Sierra Grande, Río Negro: ¿Una Nueva Unidad Cambro - Ordovícica?. 18 Congreso Geológico Argentino, Digital Proceedings. Buenos Aires.

Naipauer, M., Sato, A.M., González, P.D., Chemale Jr., F., Varela, R., Llambías, E., Greco, G., Dantas, E., 2010. Eopaleozoic Patagonia–East Antarctica connection: fossil and U-Pb evidence from El Jagüelito Formation. 7 South American Symposium on Isotope Geology, Digital Proceedings, 602–605. Brasília.

Pankhurst, R.J., Caminos, R., Rapela, C.W., 1993. Problemas geocronológicos de los granitoides gondwánicos de Nahuel Niyeu, Macizo Norpatagónico. In: 12 Congreso Geológico Argentino and 2 Congreso de Exploración de Hidrocarburos, vol. 4, pp. 99–104.

Pankhurst, R.J., Rapela, C.W., Loske, W.P., Fanning, C.M., Márquez, M., 2003. Chronological study of the pre-Permian basement rocks of southern Patagonia. Journal of South American Earth Sciences 16, 27–44.

Pankhurst, R.J., Rapela, C.W., Fanning, C.M., Márquez, M., 2006. Gondwanide continental collision and the origin of Patagonia. Earth-Science Reviews 76, 235–257.

Payne, J.L., Hand, M., Barovich, K.M., Reid, A., Evans, D.A.D., 2009. Correlations and Reconstruction Models for the 2500–1500 Ma Evolution of the Mawson Continent. In: Geological Society, London, Special Publications 323, 319–355.

Ramos, V.A., 2008. Patagonia: a Paleozoic continent adrift? Journal of South American Earth Sciences 26 (3), 235–251.

Ramos, V.A., 2010. The Grenville-age basement of the Andes. Journal of South American Earth Sciences 29, 77–91.

Rapalini, A.E., López de Luchi, M., Martínez Dopico, C., Lince Klinger, F., Giménez, M., Martínez, P., 2010. Did Patagonia collide against Gondwana in the Late Paleozoic? Some insights from a multidisciplinary study of magmatic units of the North Patagonian Massif. Geologica Acta 8 (4), 349–371.

Richards, P.C., Gatliff, R.W., Quinn, M.F., Williamson, J.P., Fannin, N.G.T., 1996. The geological evolution of the Falkland Islands continental shelf. In: Storey, B.C., King, E.C., Livermore, R.A. (Eds.), Weddell Sea Tectonics and Gondwana Breakup. Geological Society London, Special Publications 108, pp. 105–128.

Riley, T.R., Leat, P.T., Pankhurst, R.J., Harris, C., 2001. Origins of large volume rhyolitic volcanism in the Antarctic Peninsula and Patagonia by crustal melting. Journal of Petrology 42, 1043–1065.

Rolando, A.P., Hartmann, L.A., Santos, J.O.S., Fernandez, R.R., Etcheverry, R.O., Schalamuk, I.A., McNaughton, N.J., 2002. SHRIMP zircon U-Pb evidence for extended Mesozoic magmatism in Patagonian Batholith and assimilation of Archean crustal components. Journal of South American Earth Sciences 15 (2), 267–283.

Saini-Eidukat, B., Bjerg, E., Gregori, D.A., Beard, B.L., Johnson, C.M., 1999. Jurassic granites in the northern portion of the Somoncura Massif, Río Negro, Argentina. In: 14 Congreso Geológico Argentino, Salta, Actas 2, pp. 175–177.

Santos, J.O.S., Hartmann, L.A., Bossi, J., Campal, N., Schipilov, A., Piñeiro, McNaughton, N.J., 2003. Duration of the Trans-Amazonian Cycle and its correlation within South America based on U-Pb SHRIMP geochronology of the La Plata craton, Uruguay. International Geology Review 45, 27–48.

Scherer, E., Münker, C., Mezger, K., 2001. Calibration of the Lutetium–Hafnium Clock. Science 293 (5530), 683–687.

Schilling, M.E., Carlson, R.W., Conceicao, R.V., Dantas, C., Bertotto, G.W., Koester, E., 2008. Re-Os isotope constraints on subcontinental lithospheric mantle evolution of southern South America. Earth and Planetary Science Letters 268, 89–101.

Schilling, M., Tassara, A., 2008. Are the Falkland Plateau and the Deseado Massif part of the same Mesoproterozoic lithospheric block? 7th International Symposium on Andean Geodynamics (ISAG 2008, Nice), Extended Abstracts, 496–499.

SEGEMAR, 2005. Aeromagnetic Survey of Valcheta Area. Servicio Geológico-Minero Argentino, Argentina, Digital data.

Tankard, A.J., Welsink, H., Aukes, P., Newton, R., Stettler, E., 2009. Tectonic evolution of the Cape and Karoo basins of South Africa. Marine and Petroleum Geology 26 (8), 1379–1412.

Taylor, G.K., Shaw, J., 1989. The Falkland Islands: new palaeomagnetic data and their origin as a displaced terrane from southern Africa. In: Hillhouse, J.W. (Ed.), Deep structure and Past Kinematics of Accreted Terranes. American Geophysical Union, Geophysical Monograph 50, pp. 59–72.

Thomas, R.J., Jacobs, J., Eglinton, B.M., 2000. Geochemistry and isotopic evolution of the Mesoproterozoic Cape Meredith Complex, West Falkland. Geological Magazine 137 (5), 537–553.

Uriz, N.J., Cingolani, C.A., Chemale Jr., F., Macambira, M.B., Armstrong, R., 2010. Isotopic studies on detrital zircons of Silurian–Devonian siliciclastic sequences from Argentinean North Patagonia and Sierra de la Ventana regions: comparative provenance. International Journal of Earth Sciences. http://dx.doi.org/10.1007/s00531-010-0597.

Varela, R., Basei, M.A.S., Cingolani, C.A., Siga Jr., O., Passarelli, C.R., 2005. El Basamento Cristalino de los Andes norpatagónicos en Argentina: geocronología e interpretación tectónica. Revista Geológica de Chile 32, 167–182.

Veevers, J.J., Belousova, E.A., Saeed, A., Sircombe, K., Cooper, A.F., Read, S.E., 2006. Pan-Gondwanaland detrital zircons from Australia analysed for Hf-isotopes and trace elements reflect an ice-covered Antarctic provenance of 700–500 Ma age, TDM of 2.0–1.0 Ga, and alkaline affinity. Earth-Science Reviews 76, 135–174.

von Gosen, W., 2003. Thrust tectonics in the North Patagonian massif (Argentina): implications for a Patagonian plate. Tectonics 22 (1), 1005. http://dx.doi.org/10.1029/2001TC901039.

Wareham, C.D., Pankhurst, R.J., Thomas, R.J., Storey, B.C., Grantham, G.H., Jacobs, J., Eglington, B.M., 1998. Pb, Nd, and Sr isotope mapping of Grenville-age crustal provinces in Rodinia. Journal of Geology 106, 647–659.

Zappettini, E.O., Chernicoff, C.J., 2011. Arqueano a Mesoproterozoico Superior en Patagonia: evidencias de un basamento cratónico no expuesto. 18 Congreso Geológico Argentino, Digital Proceedings.